
**ATOMISTIC MODELLING TO STUDY BCC CRYSTAL
STRUCTURE OF NIOBIUM**

A DISSERTATION

Submitted in partial fulfilment of the
Requirement for the award of the degree
Of

MASTER OF TECHNOLOGY

IN

MECHANICAL AND INDUSTRIAL ENGINEERING

(WITH SPECIALIZATION IN CAD, CAM & ROBOTICS)

By

Anil Kumar Gautam (14538002)

Under the guidance of

Dr. Avinash Parashar

Assistant Professor



May 2016

**DEPARTMENT OF MECHANICAL AND INDUSTRIAL
ENGINEERING**

INDIAN INSTITUTE OF TECHNOLOGY, ROORKEE

ROORKEE-247667

CANDIDATE'S DECLARATION

I hereby declare that the work carried out in dissertation entitled, “*Atomistic Modelling to Study bcc Crystal Structure of Niobium*”, is presented on behalf of partial fulfilment of the requirements for the award of degree of “Master of Technology” in Mechanical Engineering with specialization in CAD, CAM & ROBOTICS submitted to the Department of Mechanical and Industrial Engineering, Indian Institute of Technology, Roorkee, under the guidance of Assistant Professor **Dr. Avinash Parashar** Department of Mechanical and Industrial Engineering. I have not submitted the record embodied in this report for the award of any other degree.

Date: May, 2016

Anil Kumar Gautam

Place: Roorkee

Enrolment no: 14538002

This is to certify that the above statement made by the candidate is correct to the best of my knowledge and belief.

Dr. Avinash Parashar

Assistant Professor

MIED

IIT Roorkee

ACKNOWLEDGEMENT

I am deeply indebted to my guide **Dr. Avinash Parashar**, Assistant Professor in the department of Mechanical and Industrial Engineering, Indian Institute of Technology, Roorkee, whose help, stimulating suggestions and encouragement helped me in all the time to make my effort successful.

I am also grateful to **Dr. Dinesh Kumar**, Professor and Head, and all faculty members and staff of MIED, Indian Institute of Technology, Roorkee.

I extend my thanks to all my friends who have helped directly or indirectly for the completion of this research proposal.

Finally, I would like to express my deepest gratitude to the Almighty for showering blessings on me. I gratefully acknowledge my heartiest thanks to all my family members for their inspirational impetus and moral support during the course of work.

Anil Kumar Gautam
Enrolment No.: 14538002
CAD, CAM & ROBOTICS
M.Tech IInd YEAR

Abstract

In this work atomistic modelling of bcc crystal niobium is done in order to validate the various properties of bcc crystal using molecular dynamics approach and also effect of radiation induced damages at atomistic level are widely discuss . These days' researchers are looking for clean source of energy and nuclear source of energy is merging as a potential substitute for conventional energy sources such as coal and gas based power plants. Niobium is considered as one of the important alloying constituent for manufacturing pressure tubes fuel cladding in nuclear industry. So for majority of research in nuclear materials is focused around zirconium, whereas literature is almost mute with respect to niobium. An attempt has been made by this work to present the current state of art in modelling nuclear materials such as niobium.

TABLE OF CONTENTS

1. Candidate's Declaration	i
2. Acknowledgement	ii
3. Abstract.....	iii
4. List of tables	v
5. List of figures.....	vi
6. INTRODUCTION	1
1.1 Radiation Damage and Phenomena	2
1.2 A Radiation Damage Cascade	3
1.3 Atoms and Ions interaction	9
1.4 The displacement of atoms	9
1.5 Displacement probability	9
1.6 Displacement energy.....	9
1.7 Molecular Dynamics Based Computer Simulations for Radiation Damage... 11	
1.8 Radiation Damage on Niobium	12
1.9 Definition of the problem.....	12
1.10 Niobium and its usefulness properties	13
1.11 Applications of Niobium.....	14
1.12 Natural Abundance	15
1.13 Niobium as a nuclear material	15
1.14 Literature review	16
1.15 Recent works on Molecular Dynamics based atomic simulations.....	20
7. MATHEMATICAL MODELLING TECHNIQUES FOR NIOBIUM	21
2.1 Basic concepts of Molecular Dynamics simulation.....	21
2.2 Equation of motion	24
2.3 Temperature control.....	25
2.4 Pressure control.....	26
2.5 Molecular Dynamics ensembles	27
2.6 EAM Potential	29
2.7 Validation of EAM Potentials.....	31
2.8 Effect of temperature on behavior of Niobium.....	35
2.9 Effect of simulation box.....	36
8. EFFECT OF DEFECT ON MECHANICAL PROPERTIES OF NIOBIUM.....	31
3.1 Ballistic Phase.....	38
3.2 Relaxation Phase	39
3.3 Effect of irradiation on Niobium.....	39

3.4	Combined Radiation and loading.....	48
9.	CONCLUSION.....	52
10.	REFERENCES.....	53-55

LIST OF TABLES

Table No.	Name	Page No.
1.1	Time-Scale for the Various Events/Defects in Irradiated Material	2
1.2	Properties of Niobium	13
1.3	Properties of Niobium (EAM)	13
2.1	validation of Young's Modulus by varying simulation temperature	33

LIST OF FIGURES

Figure No.	Figure Name	Page No.
1.1	Schematic representation of various stages of evolution of displacement cascades	5
1.2	Collision between two spherical balls and their velocity vectors after collision.	7
1.3	The probability of displacement as a function K.E. to lattice atom	10
1.4	Wide variety of applications of Niobium(23%) based alloy ‘Gum metal’	14
1.5	Failure cross section after tensile loading	16
1.6	Stress-strain response of Nb metal under tensile loading condition.	17
1.7	Stress-strain behaviour of Nb metal at various sizes of naopillars	18
1.8	Stress-strain behaviour of Nb metal at various sizes of naopillars.	18
2.1	Schematic representation of MD simulations	24
2.2	Change in positions and velocities of atoms with time, the changes are marked only for one atom	25
2.3	Schematic representation of various steps involved to calculate the state of atoms in MD simulations	27
2.4	Graphical representation of constant NVE, NVT and NPT ensemble	28
2.5	Simulation box with two atoms (OVITO)	32
2.6	Strain energy vs strain graph in order to validate EAM potential	33
2.7	Strain energy variation w.r.t to simulation box temperature. (Data collection from LAMMPS dump files all simulations were carried out at NPT ensemble)	34
2.8	Stress-strain graph at different temperature conditions	35
2.9	Stress-strain graph by varying simulation box size	37
3.1.1	Vacant sites at four stages in the evolution of 1 keV cascade in Niobium at 300 K.	38
3.1.2	Frenkel pairs w.r.t. different time steps	39

3.2	Defective atomic sites generated in molecular dynamics based simulation with respect to simulation box temperature	40
3.3	Distribution of defective atomic sites in the simulation box with respect to a different simulation temperatures of 3000°K, 450°K and 600°K.	41
3.4	Distribution of defective atoms at different PKA direction	42
3.5	Stress-strain response at different PKA direction (p2 stands for stress in GPA at corresponding PKA direction)	43
3.6	Distribution of defective atomic sites in the simulation box with respect to PKA velocity vector aligned with different crystal orientations at a constant temperature 300 K.	44
3.7	Defect distribution and activated slip planes at the onset of plasticity in simulations performed with different PKA directions	45
3.8	Distribution of defective atomic sites in the simulation box with respect to PKA energy	46
3.9	Distribution of defective atoms at different PKA energy.	47
3.10	Activated slip planes at the onset of plasticity in simulations performed with different PKA energy level at a constant temperature 300K.	48
3.11	Distribution of defective atomic sites in the simulation box (a) distribution of interstitials when uniaxial tensile load is applied and vacancies in (b) distribution of interstitials (c) and vacancies(d) in case only of no external loading	50
3.12	Dislocation channelling and activated slip planes at the onset of plasticity in simulations	50
3.13	Number of Frenkel pairs when Niobium single crystal is subjected to uniaxial tensile loading at PKA energy 1 keV and at 300 K temperature	51

Abbreviations

MD	Molecular dynamics
EAM	Embedded atom method
LAMMPS	Large scale atomic/molecular massively parallel simulator
VMD	Visual molecular dynamics
Zr	Zirconium
Nb	Niobium
GPa	Giga Pascal
MRI	Magnetic resonance imaging
DCM	Dynamic contact module
keV	Kilo electron volt
ps	picosecond
BCA	Binary collision approximation
EOMs	Equation of motions
NSL	Newton's second law
KMC	Kinetic Monte Carlo method
BCC	Body centred cubic
nm	nanometre
BNNS	Boron nitrides nanotubes
MM	Molecular mechanics
NPT	Number of particles, pressure and temperature
NVE	Number of particles, volume and energy
NVT	Number of particles, volume and temperature

Chapter 1

1. Introduction

In the past few years nuclear power has been emerged as a clean source of energy. Researches have done significant amount of work to understand the failure mechanism of nuclear materials such as Zirconium. Zirconium based alloys have been widely used as fuel cladding and in pressure tubes in nuclear industry. Niobium is the main constituent of Zr alloy (1-95% Zr, 2.5 % Nb, other Tin, Fe, Cr, Ni).

Niobium plays an important role when alloyed with Zr and used for cladding fuel rods and pressure tubes. Nb is having some excellent properties that make it attractive for various fields. Because of its superior mechanical properties and low neutron absorption capacity, niobium is considered as an important constituent for alloys used for cladding fuel rods and pressure tubes in nuclear reactors [1]. It is very important to understand the stability of materials subjected to irradiation and high priority task for the nuclear industry. To accomplish the aim of constructing the next generation of nuclear reactors substantial material selection, development, and performance evolution are essential. In nuclear industry material degradation put potential limit in the various reactor designs. So, far an efficient and long lasting nuclear reactor all these parameters are considered. For a material going to be used for nuclear industry as fuel cladding and pressure tubes, it must be in a position to sustain damages caused by irradiation, pressures and temperatures as compared to traditional reactors.

In nuclear industry a material which is going to be used as pressure tubes or for fuel cladding must have following properties –

- a) Low thermal neutron absorption cross-section
- b) High hardness
- c) High Ductility
- d) Corrosive resistant

Nb based alloys are promising candidate materials and used for a wide variety of technological applications. “Gum metal” which is a Ti based alloy, with substantial amount of Nb concentrations exhibits unique deformation behaviour and considerable properties [2]. With the help of Nb based super alloys various attempts have been done to enhance the operating temperature of turbine blades. Nb turned to be a promising candidate when alloyed with various material and has been used by different industries. In continuation of superior properties its low density, high melting point and biocompatible properties make it an attractive choice for alloy design.

1.1 Radiation Damage Phenomena ^[3]

The radiation damage phenomena is confined by the transfer of energy from core of the irradiated material to the solid and creating distribution of target atoms after finishing the event. The radiation damage phenomena is actually consists of various steps. These steps and their occurrence orders are explained below-

1. Lattice atom interaction with the energetic particles incident on the surface.
2. The kinetic energy which is going to be transferred to the lattice atom is responsible to generate PKA (primary knock on atom).
3. Atoms got displaced from their lattice site.
4. The kinetic energy is going to be transferred through the displacement of atoms and creating additional knocks-on-atoms.
5. Step 4 continued and distribution of defective atomic sites within the crystal structure is result of displacement cascade.
6. After few nanoseconds the termination of PKA (i.e. after relaxation phase, step 1 to step 5 come under ballistic phase will be explained further in chapter 3) some atoms got displaced permanently from their parental.

The radiation damage phenomena comes to an end when PKA comes to rest and responsible for creating interstitials and vacancies (point defects) these defects in the crystal lattice are further responsible for change in the various properties of the material. It is very important to note down that the complete phenomena of various events lasts only in the order of picoseconds and femtoseconds (see Table 1.1). Consecutive processes involving the development of the point defects and dislocation channelling of slip planes are illustrated as radiation damage effects.

Table 1.1 Time-Scale for the Various Events/Defects in Irradiated Material (Approximate).

Time (s)	Event	Result
10^{-16}	Transfer of energy from the incident particle	Formation of PKA displacement cascades
10^{-12}	Displacement lattice atoms by PKA	Displacement cascades
10^{-10}	Energy degradation	Frenkel pairs (stable)
10^{-7}	Defect reactions	SIA and vacancies recombination

1.2 A Radiation Damage Cascade^[3]

The evolution of radiation damage cascade introduce some of the commonly used terminology in the radiation damage field. We will focus our discussion on the concept of a radiation damage collision cascade and the various stages in its development. In Fig. 1.1 we give schematic illustrations of these different stages.

1.2.1 The Early Phases

When an energetic particle impinges on some target material (see Fig. 1.1a). This particle can penetrate a significant distance into the target material before undergoing a collision with an atom of the target. It depends upon its mass and charge upon the particle. This collision will set the target atom (known as the primary knock-on atom or PKA) in motion. The PKA atom will travel with a very high velocity in the medium (see Fig. 1.1b).

1.2.2 Ion Channelling

A very low cross-section for interaction is noticed when the PKA is having kinetic energy (~100 keV) when it is interacting with other nuclei material. In this situation particle travels larger distances inside crystal structure and it is unable to produce any significant collision. The process in which incident particle travels at larger distances in the crystal without undergoing any collision is called as ion channelling. (See fig.1.1 c). It plays an important role for damage distribution in crystalline material.

1.2.3 Sub Cascade Branching

Sub cascade phenomena is observed when the PKA kinetic energy was greater than the ~10 keV. An ion moving with this order energy will be able to impart sufficient amount of energy to its collision partner and able to form a sub cascade and it is important for simulating collision cascades. A set of several lower cascades originating from a high energy PKA (see fig1.1 e) creating branches of atom displacements.

1.2.4 The Displacement Phase

As the energy of moving PKA atom falls below 10 keV level the interactions with the surrounding atoms become strong. In this case frequent collisions will be found. There will be frequent collisions and responsible for displacement phase i.e. atom will get energy and they will switch to another by replacing atom of that position creating interstitials. Sometimes atom leave their position and occupied a new place and creating a vacant site in the lattice. There will be distribution of defects in the lattice sites. Over the time span of picoseconds (~1–10 picoseconds) the maximum number of atoms in a region of 10–100 nm in size will be displaced from their equilibrium lattice sites. (See fig.1.1 g)

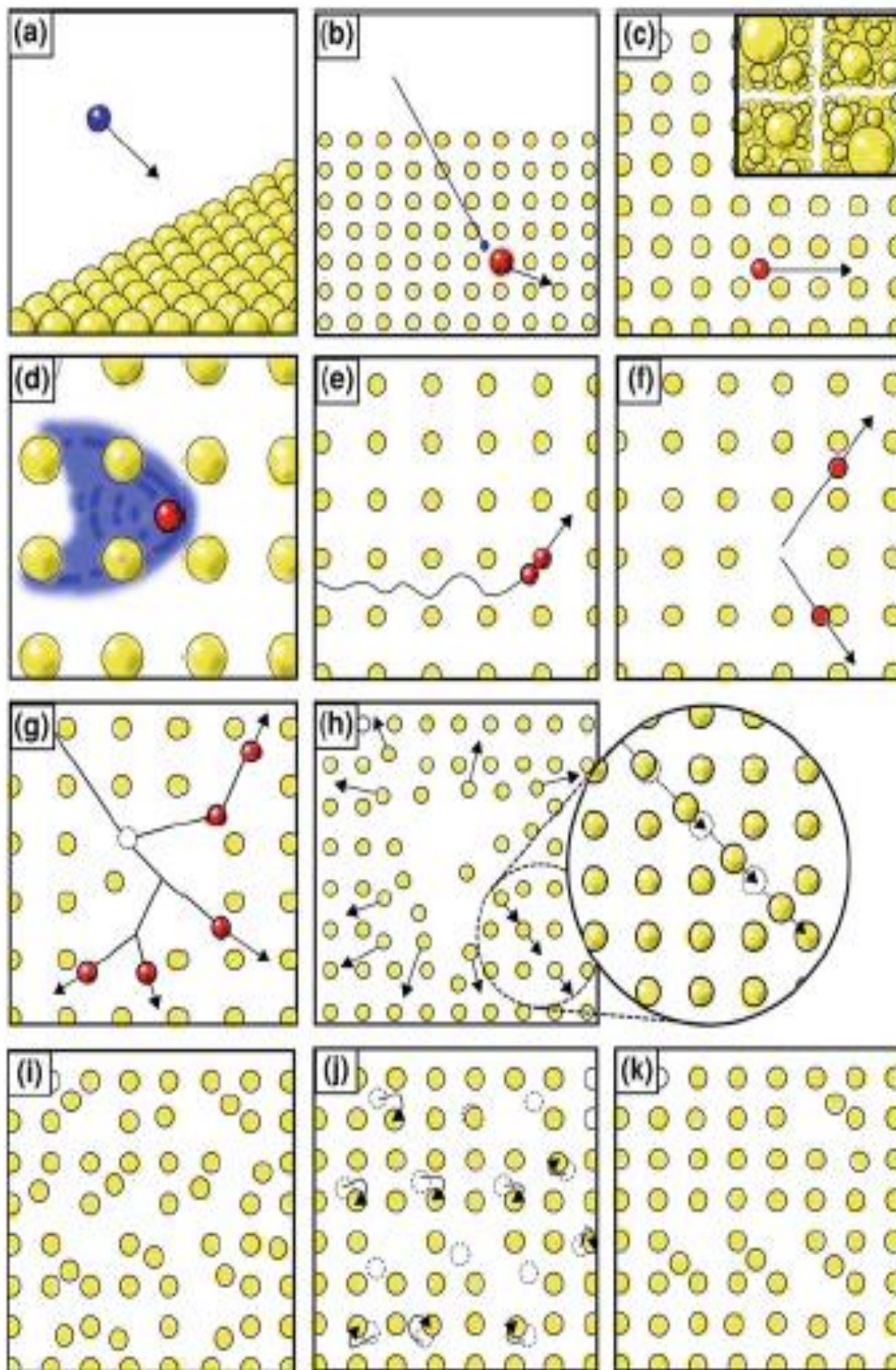


Fig.1.1 schematic representation of various stages of evolution of displacement cascades [3]

1.2.5 Thermal Spike-

This phase follows by displacement phase. Atoms are displaced from their original lattice position because of energy transferred from the incident particle. The amount of energy is now decreased and atoms cannot attain their original position. Now the relaxation phase is seen due to termination of distributed kinetic energy with time. This cascade energy rapidly distributed among all the atoms in the cascade region. In relaxation phase a hot region is formed that we called as thermal spike (see fig1.1 i). At this phase many atoms are displaced from their lattice sites and responsible for vacancies in interstitials.

After thermal spike cooling phase occurs and lasted for hundred picoseconds, at this stage thermal spike grows gradually and then cools. There is a chance of recombining interstitials and vacancy defects (see fig1.1 j).

1.2 Interaction between Neutron and Nucleus ^[3]

Neutrons are electrically neutral (there is no chance of charge transfer between neutron and interacting atom), with this property, collisions (elastic) between neutrons and nuclei can be modelled as collision between two rigid spheres. During neutrons travel through a solid there is a finite probability of neutron to collide with the lattice atom. During this elastic collision neutron transfer its energy to the struck atom and from the struck atom to another atom and so on and this process continued till the termination of PKA energy. Mathematically we can defined the finite probability of collision with the help of following equations. Its probability is defined in the equation 1&2 (as a function of energy and angle). For single scattering probability is defined as-

$$\sigma_s(E_i, E_f, \sigma) = \int \sigma_s(E_i, E_f, \sigma) dE_f \quad 1$$

The total distribution probability for neutrons of energy E_i is defined as:

$$\sigma_s(E_i) = \int \sigma_s(E_i, \sigma) d\sigma \quad 2$$

Where;

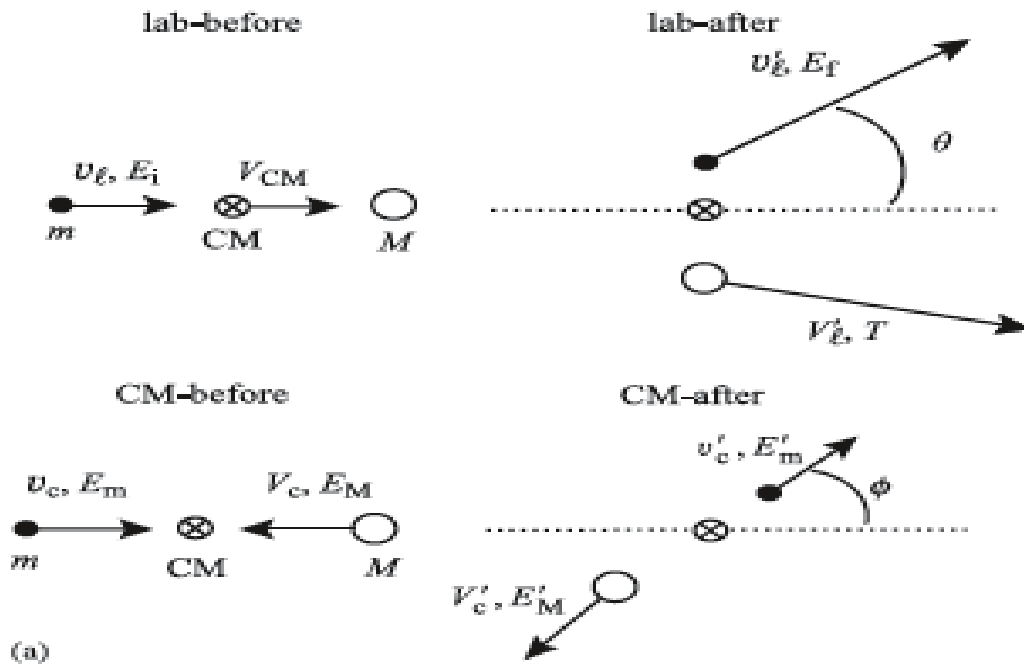
E_i =incident energy

E_f =Final energy

σ = neutron scattering solid angle

In order to understand the irradiation effects, our main concern is to analyse the behaviour of the target atom. That's why we are looking for $\sigma_s(E_i, T)$ it is the probability of a neutron energy E_i elastically going to be transfer to an atom, and it will transfer a rebound energy T to the target atom. For that first of all it is important to calculate T in terms neutron energy and the scattering angle. To analyse it binary elastic collision in the centre mass has been illustrated below.

Figure 1.2a shows paths of a neutron and the target nucleus before and after interaction. The simplest way to obtain relationship between the energy of incident particle, scattering angle and delivered energy is to analyse the dynamics of the collision in the two solid body system. (Law of momentum conservation along the axes of collision).



(a)

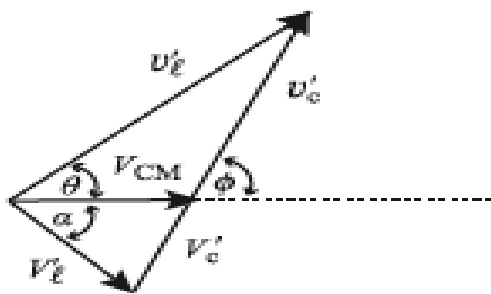


Fig1.2 velocity vector (a) collision between two spherical balls and their velocity vectors after collision, velocity triangle is shown in below diagram. [3]

Applying the law of conservation of momentum along the axis of approach and departure results;

$$v_{cm} - V_{cm} = 0 \text{ and } v_{cm'} - V_{cm'} = 0 \quad 1$$

Applying law of conservation of energy-

$$\frac{1}{2}mv_c^2 + \frac{1}{2}MV_c^2 = \frac{1}{2}v_{1'}^2 + \frac{1}{2}MV_{c'}^2 \quad 2$$

From equation 1&2;

$$\left[\frac{1}{2}m \left(\frac{m}{M} \right)^2 + \frac{1}{2}M \right] V_c^2 = \left[\frac{1}{2}m \left(\frac{m}{M} \right)^2 + \frac{1}{2}M \right] V_{c'}^2$$

And $v_c = v_{c'}$

$$V_c = V_{c'}$$

Thus we can say that the velocity of incident particle is transferred completely to the atom which was earlier in rest condition this the case of perfect elastic collision.

Similarly in the case of radiation damage the neutron generated in the nuclear reaction chain is having high kinetic energy the atoms of shielding material is at rest. Considering the case that neutron and the interacting atom is in the same direction from the above results the kinetic energy is transferred to the atom. Now interacting atom is at higher energy level. In the lattice structure atom are arranged in a perfect way. This atom will transfer its energy to the adjacent atom that atom will transfer to another atom this process will continue till the termination of kinetic energy. Atoms got disturbed from their equilibrium and responsible for displacement cascades. This whole process takes place in picoseconds displacement of atoms with time is explained in detail earlier. (See fig.1.1 displacement phase).

1.3 Atoms and Ions Interactions

Atom-atom or ion –atom collisions are interactions between electron clouds and nuclei. These interactions are explained by interatomic potentials. These potential function describe all the interactions. This interaction nature is a strong function of atom energies and their atomic distances.

1.4 The Displacement of Atoms

The energy associated with the lattice atom is let's say T , we defined it as the primary knock-on atom i.e. PKA. This high energy atom moves through the lattice and collides with the other lattice atoms and meanwhile transferring energy. It creates displacement cascades in the crystal Structure. If this collision continue, a pattern of tertiary knock-ons is generated and further resulting in collision cascades. As we defined earlier cascade is spatial distribution of lattice interstitials and vacancies. This phenomena plays an important role on the physical and mechanical properties of alloys. Our main aim is to quantify these displacement cascade. When a neutron of energy E_i striking a lattice atom, how many atoms displacement will result? We are going to develop a model in order to quantify the number of defects generated due to irradiation damage.

1.5 Displacement Probability^[3]

There is some minimum energy required to struck atom and create displacement cascade which we refer as threshold energy E_d . We define $P_d T$ as the probability that a struck atom is going to be displaced upon incident of energy T . The magnitude of this minimum energy depends upon crystallographic structure of the lattice, the orientation of the incident PKA, the thermal energy associated with the lattice atom, etc. Model for the displacement probability is defined as step function:

$$P_d(T) = 0 \text{ For } T < E_d$$

$$P_d(T) = 1 \text{ For } T > E_d$$

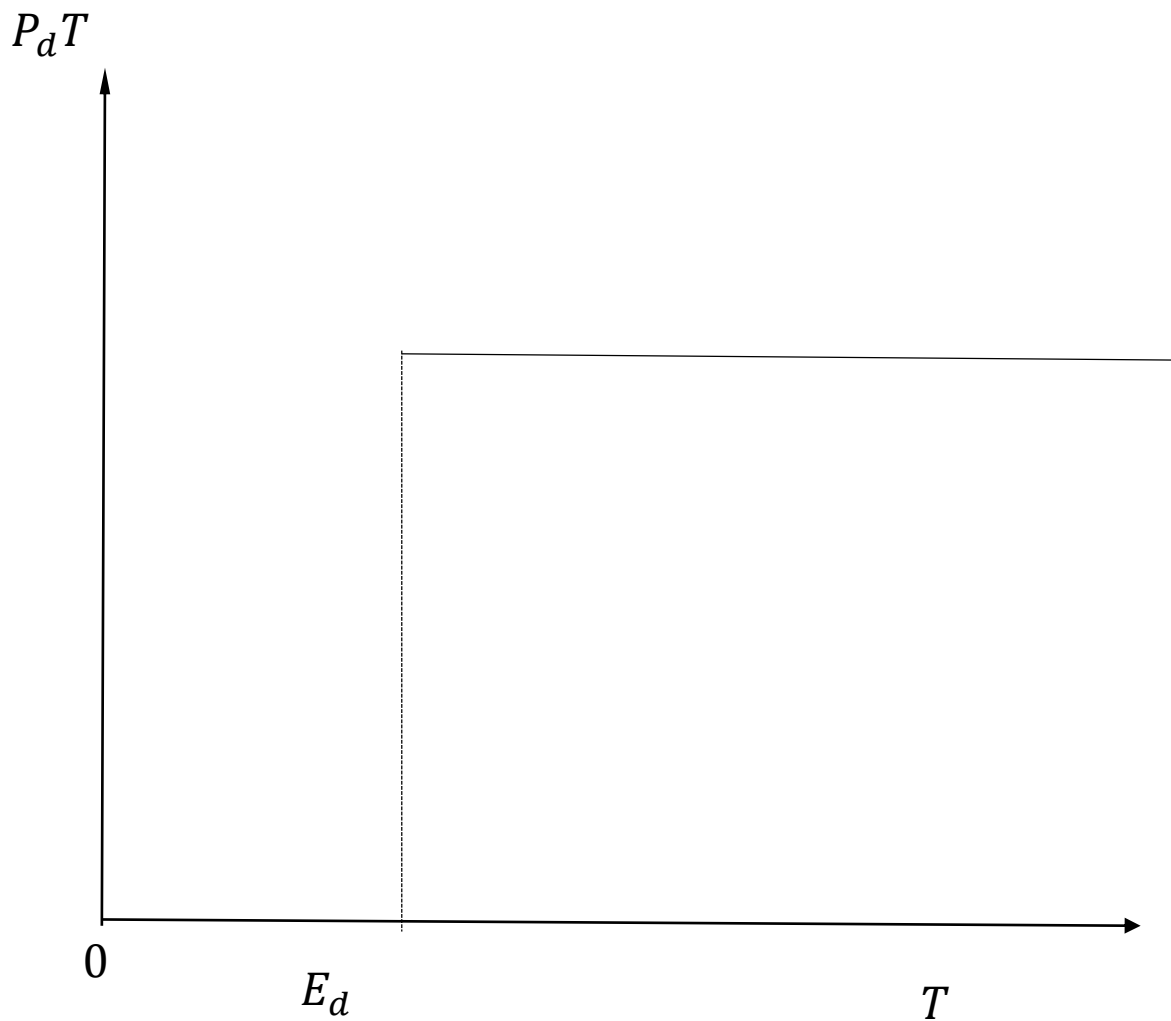


Fig1.3 the probability of displacement as a function K.E. to lattice atom

1.6 The Displacement Energy

Minimum amount of energy is required in the collision process in order to create displaced atom from its lattice site. This minimum amount of energy is called as displacement threshold or displacement energy E_d . As we discussed earlier if the energy transferred, T , is less than minimum level (i.e. E_d) the struck atom will not be displaced but only vibrate at its equilibrium position. These vibrations will be further transferred to adjacent atoms through their potential field interaction and after some time energy will appear as heat.

Hence the potential fields associated with the lattice atoms create a barrier, the struck atom must overcome this barrier of energy which we also call as threshold energy in order to get displaced.

1.7 Molecular Dynamics Based Computer Simulations for Radiation Damage^[4]

To understand the damage caused by an energetic particle incident on target analytical solutions were widely applied. Later on with the development excellent equipment's exists to analyse the defect clusters such as x-Ray scattering, small angle neutron scattering, positron annihilation spectroscopy and transmission electron microscopy. But these instruments not in a position to give to give the perfect resolution for each defects and are unable to capture the temporal development of the cascade. We must turn to computer simulations for a better understanding of spatial and temporal development of cascade.

Computer based modelling techniques are classified as-

- 1.) Binary collision approximation(BCA) method
- 2.) Molecular dynamics method and
- 3.) Kinetic Monte Carlo method.

(Note- above methods are further discussed in detail in chapter 2 mathematical modelling techniques)

1.) Binary collision approximation(BCA) method

As the name suggests, interactions between two colliding atoms is going to be taken into consideration at a time and in sequence. Only atoms having considerable energy are taken for computation. It neglects the many body interactions and hence provides a good approximation at collision stage. If energies are near or even less than the displacement energy, with the help of BCA calculations one can easily analyse the ballistic features of cascades.

2.) Molecular dynamics method

Molecular dynamics technique is on of major the techniques and widely used to describe the collision cascade. It gives the most realistic explanation of atomic interactions in the cascade. It uses realistic interatomic potentials and suitable boundary conditions. The analytical interatomic potential functions describes the force on an atom as a function of the distances between atoms in the system. In molecular dynamics simulations the total amount of energy of the system of atoms is simulated and calculated by adding over all the atoms. The forces between the atoms are used to calculate the acceleration of atoms with the help of NSL (Newton's second law);

$$F = ma$$

And by integrating acceleration equations, EOMs (equation of motions) for atoms are obtained, with these equations are further numerically solved by computer based codes or algorithms over a very small time steps. The process of numerical integration till the required state is achieved. Very small time step in MD simulations are used (i.e. of order of picosecond and femtoseconds).

3.) Kinetic Monte Carlo method

In order to simulate the dynamical evolution of system of atoms during displacement cascade molecular dynamics is used and it provides suitable results. By integrating the classical EOMs forward in time and we found the behaviour of system naturally. But in MD simulations we generally used very small time steps ($\sim 10^{-15}$ s) for accurate integration. This method offers a dynamically correct trajectories through space and time and total time for integration is limited to order of nanoseconds. It puts limit in order to study diffusion and annihilation of defects after cascade events. These events are of longer time-scales (relatively) and creates a time-scale problem .so the KMC method is an attempt to overcome this time-scale problem.

1.8 Radiation Damage on Niobium

Defect generation in nuclear materials due irradiation significantly affects the microstructure of such materials. Defect generated due to cascade mechanism in bcc crystal structure is of major concern for materials performance in power reactors because Nb based alloys are widely used in the nuclear industry. Due to radiation damage cascades creates in crystal structure basically in two phases ballistic phase and relaxation phase, crystal structure effects by the cascades mechanism, either in the early ballistic phase or in the consecutive period of relaxation phase. At relaxation phase thermal spike defects are significant. Irradiation temperature significantly effects the evolution of radiation damage in alloys and metals. The energy imparted duration due to radiation on the material is of nanoseconds and femtoseconds. Motion of defects and formation of dislocation channelling slip planes takes place because of radiation damage on Niobium.

1.9 Definition of the problem

Atomistic modelling to study bcc crystal structure of Niobium. Niobium is plays an important role when alloyed with the Zr and widely used by nuclear industry and so far significant amount of work has been done on the Zr to understand the failure mechanism due to irradiation

damage. Niobium plays as an important role for cladding fuel rods and pressure tubes in nuclear industry so this work will add some important results to predict the failure mechanism of Nb crystal at atomistic level.

1.10 Niobium and its Usefulness/Properties

Superior mechanical properties of niobium [5] (Zr), such as low thermal neutron absorption cross section, high hardness, ductility and corrosion resistance make it an attractive material for nuclear industries. Due to its low density, high melting temperature and biocompatible properties it is widely used for alloy design in various industries [6]. Niobium material based super alloys used in the hot section of aircraft and gas turbine engines to provide them creep strength.

Tableno.1.2 Properties of Niobium-

Young's modulus(E)	106 GPa
Shear modulus(G)	37 GPa
Bulk modulus(K)	172 GPa
Thermal conductivity(ρ)	53.7 Wm ⁻¹ K ⁻¹
Poisson's ratio(μ)	0.40

To validate the EAM potential simulations were performed at NPT ensemble and at a temperature 300 K (will be explained further in chapter 2) the following properties were estimated with the help Molecular dynamics and compared with the tabulated data in paper [7].

Tableno.1.3 Properties of Niobium (EAM)

S.No.	Property	Value
1.	Lattice constant	3.308 Å
2.	Cohesive energy	7.09 eV/atom
3.	Young's modulus	115.4 GPa

1.11 Applications of Niobium

Niobium based alloys are widely used to fulfil some specific properties. Addition of Niobium in metal improves the strength of the alloys, especially at low temperatures. Niobium based alloys are not only used in nuclear industry but also used in aircraft industry such as jet engines and rockets. In architecture design to make beams and girders, Niobium based alloys are also used to make oil and gas pipelines and it increased the pressure carrying capacity of the pipes [8].

Niobium alloys are having a wide variety of technological applications. ‘Gum metal’ (23% Nb) is a multifunctional Ti based alloy [9]. It contains remarkable properties and unique deformation behaviour. Gum metal is used in aerospace industry, in making of automobile parts, robotics parts, creating artificial bones, sports goods and precision machining parts that’s why it is called as multifunctional alloy. Nb plays an important role to make gumetal multi-function-

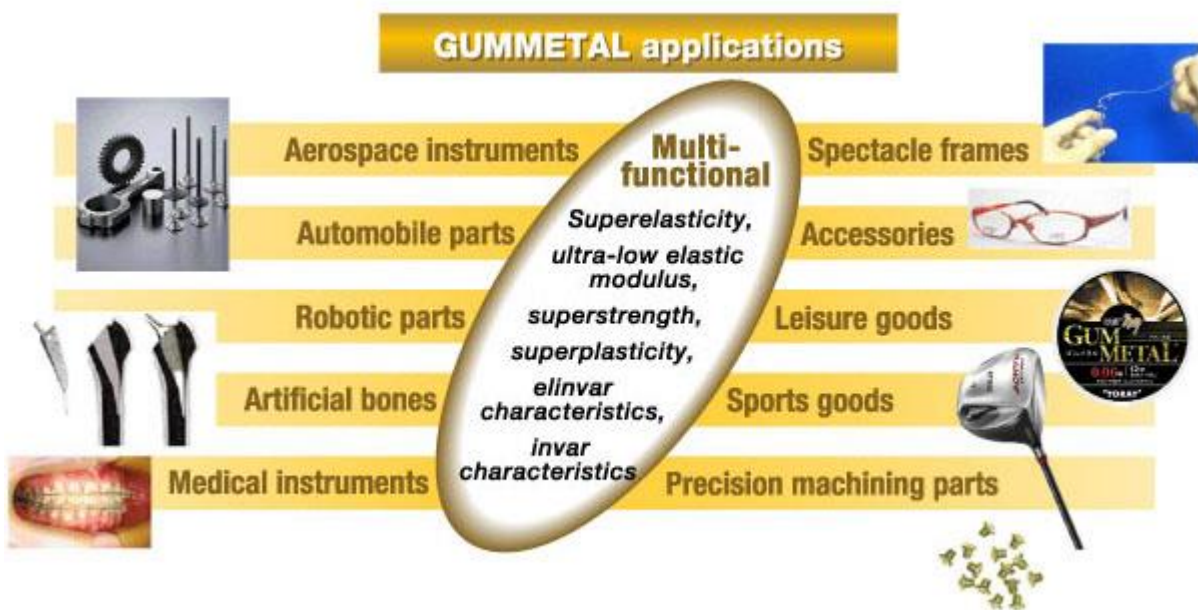


Fig.1.4 wide variety of applications of Niobium (23%) based alloy ‘Gum metal’ [9]

-al alloy. Nb based alloys are used in superconducting materials, electronics, optics, numismatics (making of coins) and jewellery [10]. Niobium is used as a basis material for various barium titanate compositions. These alloys are further used as dielectric coatings in telecommunications. Some applications in electronics fields, such as cell phones, pagers and

laptop computers. Niobium is also used in medical field for research applications [11].

The most important application for niobium is as an alloying element. It enhances the strength of high-strength-low-alloy steels. These alloys are used to build automobiles and high pressure gas transmission pipelines [12].

Niobium is also applied in stainless steel automobile exhaust systems and for the manufacturing of superconducting niobium-titanium based alloys. Nb-Ti based alloys are used to build MRI (magnetic resonance imaging) magnets [13]. MRI magnets allows corrective glasses to be made with thinner lenses.

1.12 Natural Abundance

The main source of Nb is the mineral columbite (an ore of niobium). This mineral also contains tantalum and the two elements are mined together. Columbite ^[14] is mainly found in Canada (~10%), Brazil (~80%), (10% others) such as Australia, Nigeria and elsewhere. Another method to produce Nb as a by-product of tin extraction.

1.13 Niobium as nuclear material when alloyed with zirconium

As we discussed earlier some of its properties which makes it an attractive and promising material for nuclear industry. When Nb is alloyed with Zr (~2.5% Nb) ,alloy becomes suitable for the application of nuclear industry as in cladding fuel rods and pressure tubes. Because of its extraordinary properties it has been used by nuclear industry since past few decades.

1.14 LITERATURE REVIEW

1.14.1 Tensile and Compressive Behaviour of Niobium:

The mechanical behaviour of body-centered-cubic (bcc) metals has been studied widely. BCC metals are having high strengths and high melting temperatures. These properties make them attractive for various industries. They are widely used in various tensile and compressive loading applications. The stress-strain relationship in bcc metals have a strong temperature dependence, strong strain-rate dependence and strong orientation dependence. BCC metals have asymmetry in tension and compression test. This behaviour is because of their unusual slip behaviour.

The tension tests for Nb material has been conducted in a custom-built in situ mechanical tester [15]. In fig.1.5 image of niobium cross section after applied tensile load.

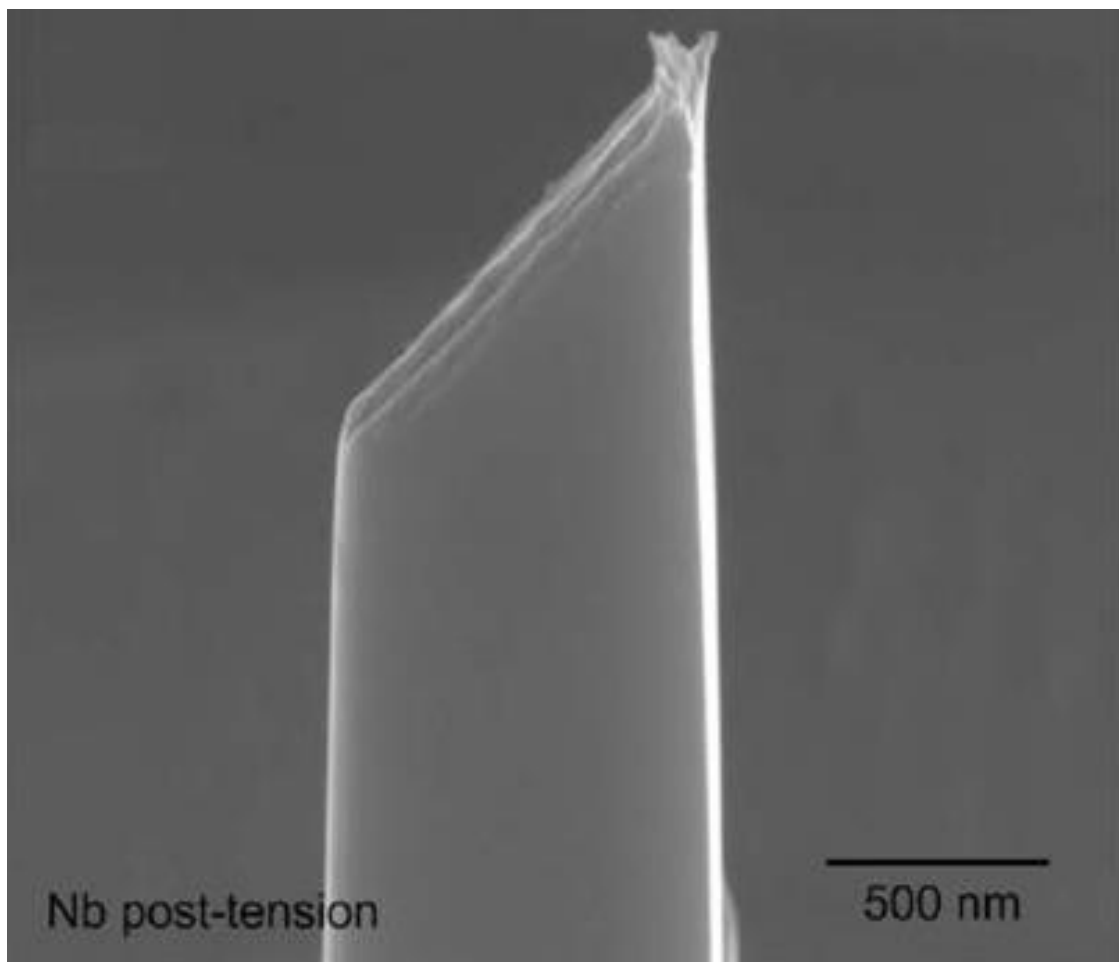


Figure 1.5 failure cross section after tensile loading is shown above [16]

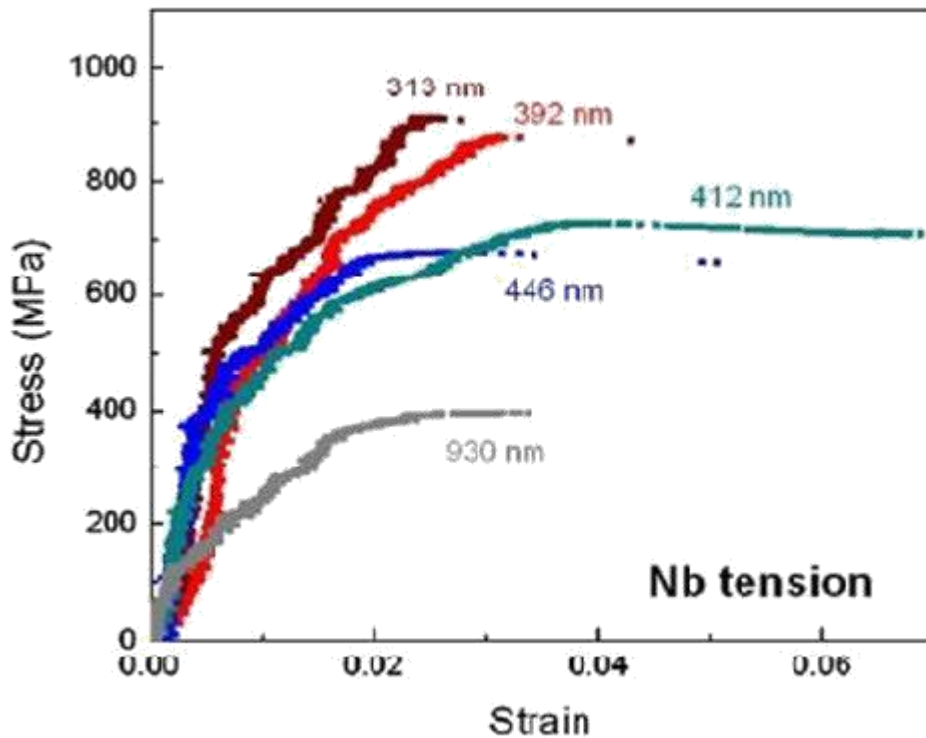


Figure 1.6 stress-strain response of Nb metal under tensile loading condition. For this various sizes of nanopillars are used size range 200nm to 1000nm. [16]

Important Points

To conduct tension test on Nb material various sizes of niobium metals has been taken. These tests were conducted to notify the behaviour of niobium material at atomistic level by keeping cross-section shape constant and varying size. The cross-section of specimen was circular and effective diameter size range from 200 to 1000 nm. Stress-strain response has been shown in fig.1.6. From the fig.1.6 it is noticed that area under the stress-strain curve i.e. toughness is maximum at 430 nm size nanopillar. It increase with increase in nano pillar size and vice versa. Yield point is maximum at 313 nm nano pillar size.

Nano pillars with circular cross-sections for compression and diameters [17] between 200 and 900 nm and tension samples with rectangular cross-sections and effective diameters between 250 and 1000 nm.

The compression tests has been conducted in the lab with the help of dynamic contact module. (ref a). Fig.1.7 is showing the image of 500 nm niobium nanopillar cross-section under compressive loading. Stress-strain response has been shown in fig1.8.

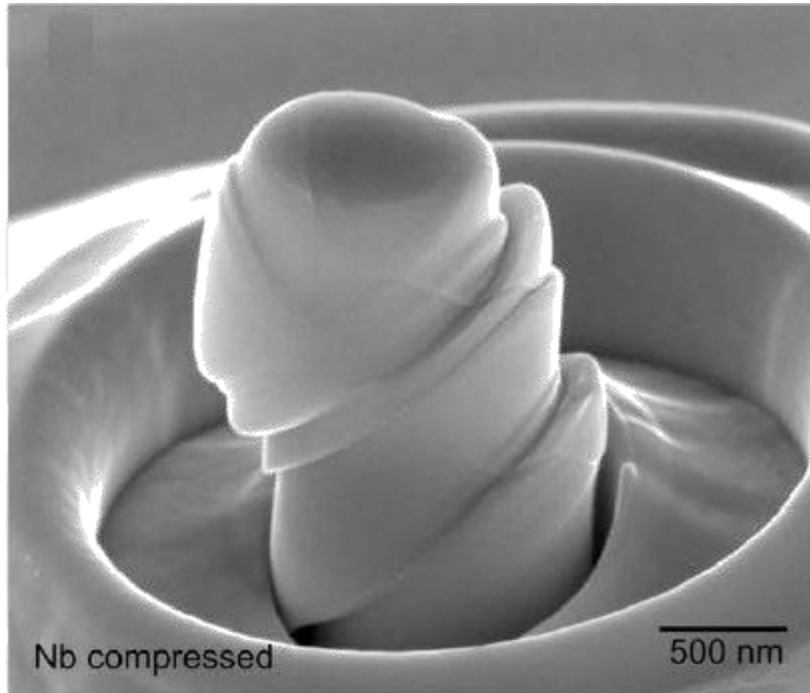


Figure 1.7 stress-strain behaviour of Nb metal at various sizes of nanopillars. [17]

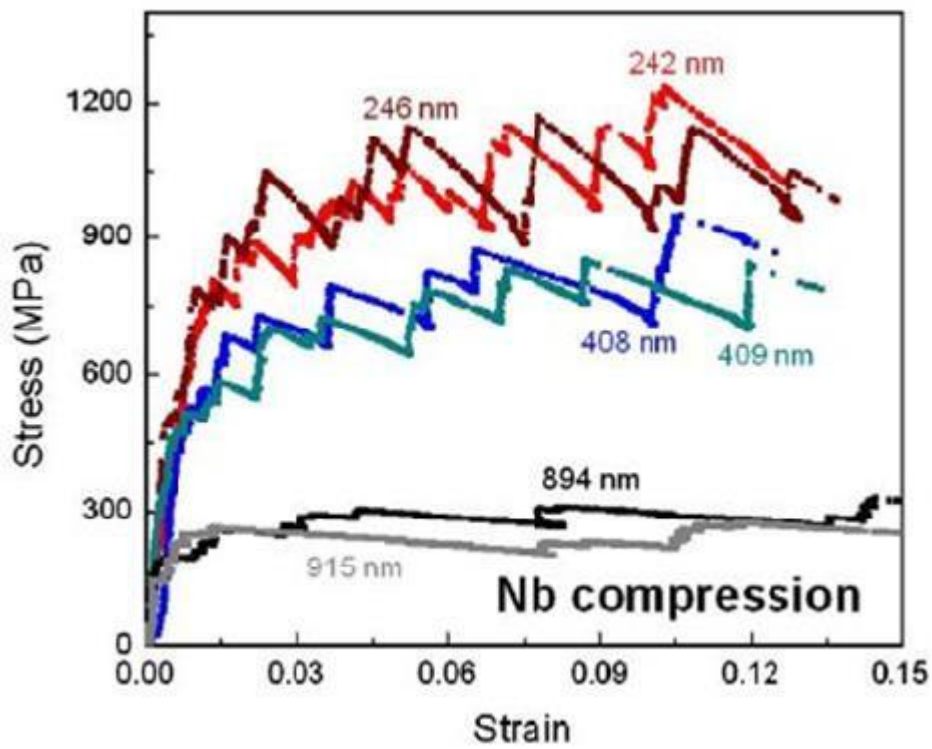


Figure 1.8 stress-strain behaviour of Nb metal at various sizes of nanopillars. [17]

Important points

- Niobium exhibits size effects on its properties i.e. in compression as well as in tension.
- Different flow stress at different sizes i.e. compression shows size effect in flow stress
- Most of the reloading segment appears elastic in nature, after that strain hardening starts.
- Plastic deformation regions are having some strain bursts this the result of strong gripping constraint in tension.

Molecular Dynamics Based Study of High Energy Displacement in α -Zirconium^[18]

Important results have been noticed from the literature of α -zirconium, in which molecular dynamics based investigation has been performed.

- Displacement cascades have been simulated at various PKA energies (~20 keV) in α -zirconium.
- Displacement cascades are varying with PKA energy and plays an important role in the final distribution of defective atomic sites.
- Temporary displacement of atoms in ballistic phase having more probability of creating defective atomic (i.e. Frenkel Pairs) sites and lower probability of creating defect clusters.
- The defect production efficiency decrease as the energy of PKA atom decreases with time, this phase we refer as relaxation phase.
- Interstitials and vacancies created in the cascade process.

Temperature Dependence of Defect Creation and Clustering by Displacement Cascades in α -Zirconium^[19]

- A molecular dynamics based investigation has been carried out to understand the primary damage process on displacement cascades with energy up to (~20 keV).
- The effect of temperature on the thermal spike has been studied. The number of Frenkel pairs has been quantified and various effects has been observed
- Number of Frenkel pairs decrease with increasing temperature for a given cascade energy. The life time of thermal spike increases with temperature.
- Size and number of Frenkel pair's increases with increasing energy.

- Clusters formed during simulation containing 25 interstitials and 24 vacancy in zirconium by 20 keV cascades at 600 K temperature.

1.15 Recent Works on Molecular Dynamics Based Atomistic Simulations

Following are some important works that has been done recently on molecular dynamics based atomistic simulation –

Rajesh Kumar, G Rajshekharan and Avinash Parashar (2016) [20]

Molecular dynamics based study on boron nitrides nanotubes (BNNS) to see the behaviour of material at tensile loading at atomistic level.

G Rajshekharan and Avinash Parashar (2016) [21]

They revealed the mechanical response and failure behaviour of graphene. And suggested performance enhancement via 5-7-7-5 (pentagon-heptagon-heptagon-pentagon). The work concluded that the mechanical properties and failure response is highly geometrical dependent in graphene. Their work suggested that by creating defects in the graphene sheets there is enhancement in mechanical and electronic properties. With these modifications in the basic structure of graphene sheet new functionalities are found in the graphene sheet which are not available in pristine case. Their work was based on molecular dynamics simulations by using suitable molecular mechanics (MM) potential field.

Buchler et al [22]. Develop a huge cluster of atoms by incorporating billion atoms in the simulation box for investigating the ductile material failure [22].

Namilae et al [23].

In his work he study the formation and sliding of grain boundaries in bi-crystals (symmetric tilt boundaries of Al and Mg doped Al) using molecular dynamics based simulations. The position of Mg atom effects the grain boundary energy in Al bi-crystal.

Zheng and Zhang [24]

In his work study of mechanical deformation in nano crystalline copper using molecular dynamics based simulations.

Furakay and his team [25]

Study of Inter granular fracture in nano-crystalline material, their work was also based on molecular dynamics based simulations.

CHAPTER 2

MATHEMATICAL MODELLING TECHNIQUES FOR NIOBIUM

2.1 Basic Concept of Molecular Dynamics Simulation^[26]

In the past few years with the advancement in the computational techniques, molecular dynamics simulations (MDs) have been emerged as a very useful and efficient tool to connect the predictions of theoretical models with experimental results, and also to explain many of the microscopic mechanisms behind the measured properties. The expectation of materials' properties from their chemical alignment is crucial for the improvement of products at industrial level. Molecular dynamics simulations plays an important role in the study of these materials, as they set up a very effective way not only for the computation of their macroscopic physical and chemical properties, but also for clarifying the atomistic mechanisms that determine these properties, thereby providing a link between the micro and macro levels.

The major concern of the atomistic level modelling is to analyse and understand the position variation of each atom in the particular material. Time dependent behaviour of molecular system is calculated by using molecular dynamics based simulations. Various numerical integration techniques are available to find out the position of any particle by integrating the equations of motion. In our case we are using Velocity –Verlet algorithm. (Explained in 2.2). This algorithm basically consists of following steps-

- 1) Calculation of interacting forces between systems of atoms. The atoms are interacting to each other at initial stage because of molecular mechanics based potential field is applied between the atoms.
- 2) Tracking of the atoms movement by integrating Newton's EOMs (equation of motions). and,

Molecular dynamics is basically a method of particle tracking by applying numerical integration technique. In this trajectories of system of ' N ' particles formulated by directly integrating Newton's EOMs. An important concern is to specify the suitable potential field in order to produce interatomic potential. Some suitable initial and final boundary are also

required. These conditions are important and plays an important role to achieve equilibrium condition.

“In dynamics the motion of the particles calculated by considering the cause of the motion i.e. force unlike in kinematics motion of particles or bodies are considered without considering the cause of the motion or neglecting the effect of forces in order to calculate the motion/position of particles or bodies.”

With above analogy in molecular dynamics the motion of atoms is calculated by considering the cause of the motion i.e. molecular mechanics (MM) potential field. Atoms interaction because of this MM potential field. Once the cause of motion is determined i.e. potential field, with the help of suitable numerical integration we can calculate the state of atom at any time step. Molecular dynamics (MD) is a mechanics based computer simulation method in which the time evaluation of a set of interacting atoms is followed by integrating their equation of motion. From the literature survey we concluded that three major computational techniques are available to perform molecular- level simulations;

- Molecular Mechanics (MM);
- Molecular Dynamics (MD) ;
- Monte Carlo (MC).

2.1.1 Molecular Mechanics (MM)

In the method of molecular mechanics, the properties of the system are calculated by considering first a collection of static microstructures. These microstructures are created by starting from an initial configuration where the particles are randomly arranged in the simulation box. They are typically characterized by exceedingly large values of the potential energy because of the presence of atom-atom overlaps, thus the energy should be quickly minimized for these overlaps to be removed.

2.1.2 Molecular Dynamics (MD)

The Molecular Dynamics method is based on the solution of Newton’s equations of motion and solves classical equations of motion at each step. These equations are numerically integrated and the result of the integration yields the positions and velocities of each particle or atom in the system in the course of time. In this way it is possible to study the time evolution of the simulated model system. And after system equilibration (at the prescribed temperature

or pressure conditions), one can extract all the dynamical and structural properties of the system.

2.1.3 Monte Carlo (MC) Method

In the Monte Carlo method, thermodynamic average values are calculated via stochastic sampling of a very large number of configurations of the microscopic system. Monte Carlo techniques can efficiently exceed large energy barriers, thus allowing for the fast relaxation of the simulated system. But because the system is not allowed to evolve naturally in time, this technique cannot offer any information about the dynamical behaviour of the system.

There are some benefits of molecular dynamics based simulations as compare to other mentioned technique. First of all we will discuss about molecular dynamics simulation advantage over Monte- Carlo simulations technique and are listed below-

- 1) Calculation of heat capacity (constant pressure heat capacity(C_p) and constant volume heat capacity(C_v) in case of compressible objects in case of solids and liquids single heat capacity(C) value exists),the value of compressibility factor and interfacial properties can be performed in a more efficient and accurate way.
- 2) Dynamic related quantities, such as transport coefficients (for e.g. thermal diffusivity and dynamic viscosity) and correlation functions of time, can be easily obtained by MD based simulations.
- 3) Total time frame required to run a MD simulation can be calculated easily by multiplying total number of time steps to attain relaxation stage and time step. In Monte-Carlo method simulation time calculation is comparatively more difficult. There is a thermal phase for which fine transition rules are there. These rules are not helpful to calculate the time frame taken to attain transition state or microstate. [80].

So we can conclude that the MD simulations success is highly dependent on potential field. In MD simulations the motion of atoms are treated as the motion of particles or motion of classical Newtonian particles. Real system of atoms at finite temperature is in constant motion.

$$f_i = (-) \frac{\partial E_i}{\partial r_i} \quad (1)$$

$$f_i = m_i \frac{\partial^2 r_i}{\partial t^2} = m_i a_i$$

Where; f_i = force of atom

m_i = mass of atom

\ddot{r} = acceleration of atom

$$f_i = -\frac{\partial E_i}{\partial r_i} \quad \text{Where ;}(i=1 \dots N)$$

E_i = potential energy;

r_i = position of atom

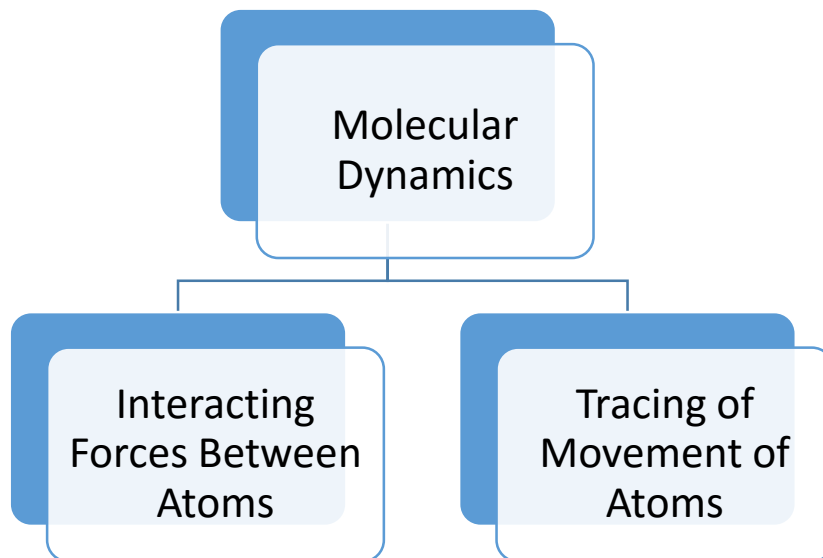


Figure 2.1 schematic representation of MD simulations

2.2 Equation of motion ^[26]

- 1.) Calculate forces between the atoms by taking the gradient of molecular mechanics potential field.

$$f_i = -\frac{\partial E_i}{\partial r_i}$$

Where E_i and r_i are the potential energy and position of atom i , respectively.

2.) Integrating force equation gives the acceleration of the atoms.

$$f_i = m_i \frac{\partial^2 r_i}{\partial t^2} = m_i a_i$$

Where m_i , r_i , and a_i are the mass, position, and acceleration of atom i , respectively

3.) By numerical integration technique, velocity and position of atoms can be calculated in a given time step. By velocity Verlet[26] method, new positions and velocities are obtained as :

$$v(t_0 + \frac{\Delta t}{2}) = (t_0 v) + a(t_0) \frac{\Delta t}{2}$$

$$r(t_0 + \Delta t) = r(t_0) + v(t_0 + \frac{\Delta t}{2}) \Delta t$$

$$v(t_0 + \Delta t) = v(t_0 + \frac{\Delta t}{2}) + a(t_0) \Delta t$$

Where r , v , and a are the position, velocity, and acceleration of an atom, respectively; t_0 is the initial time; Δt is the time step.

In MD simulations temperature and pressure control is essential which is achieved by modifying the velocities of atoms and adjusting size of simulator.

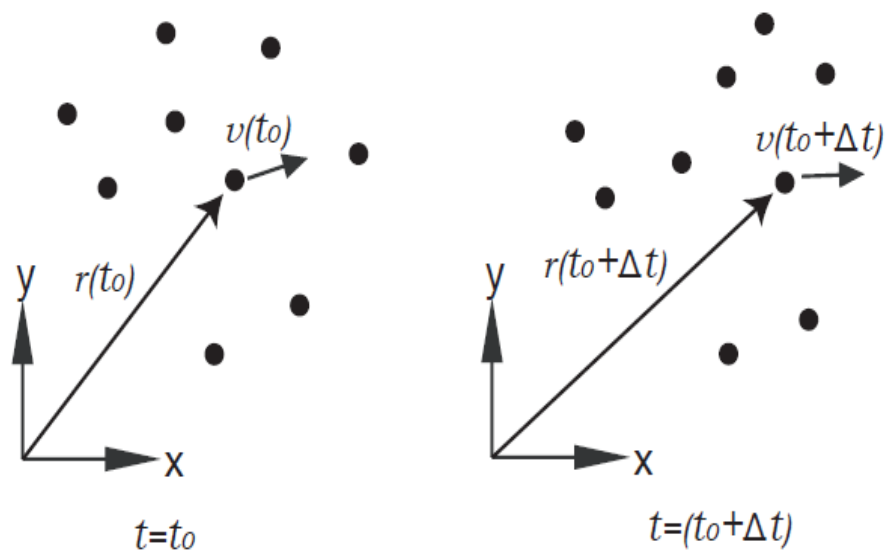


Figure2. 2 Change in positions and velocities of atoms with time, the changes are marked only for one atom [26]

2.3 Temperature Control

Temperature of a system of atoms is defined as the average of kinetic energies of all particles. The instantaneous temperature can be given as

$$T = \frac{1}{N_f K_B} \sum m_i (v_i^\alpha)^2$$

where N_f is the total translational degrees of freedom of the system, K_B is Boltzmann's constant, m_i is the mass of atom and v_i^α is the velocity of atom in i direction. The value of α can be 2 or 3 depending on the dimensionality of the system.

From the above equation it's clear that the temperature is the function of velocity and fluctuations of velocity is always there so by scaling the velocities only average value of temperature can be maintained.

Temperature control technique

Thermostat is used in order to maintain average temperature .commonly used thermostats are-

1. Anderson^[27]
2. Berendsen^[28]
3. Nose Hoover^[29]

By literature study Nose Hoover is commonly used thermostat.

2.4 Pressure Control ^[30]

The pressure of a system of atoms is defined as

$$P = \frac{1}{V} \sum_\alpha n [\sum_{\beta=1}^N i (r_i^\beta - r_j^\alpha) f_j^{\alpha\beta} + m_i^\alpha v_i^\alpha v_j^\alpha]$$

Where (i, j) are directional indices and β is an assigned number to the neighbouring atoms that goes from 1 to the number of neighbouring atoms N ; r_i^α is the position of atom α along direction i and $f_j^{\alpha\beta}$ is the force along direction j on atom α due to atom β ; m_i^α and v_i^α and are the mass and velocity of atom α , respectively. V is the total volume of the system.

Berendsen barostat and Nose-Hoover barostat are the most commonly used barostats to control pressure in MD simulations.

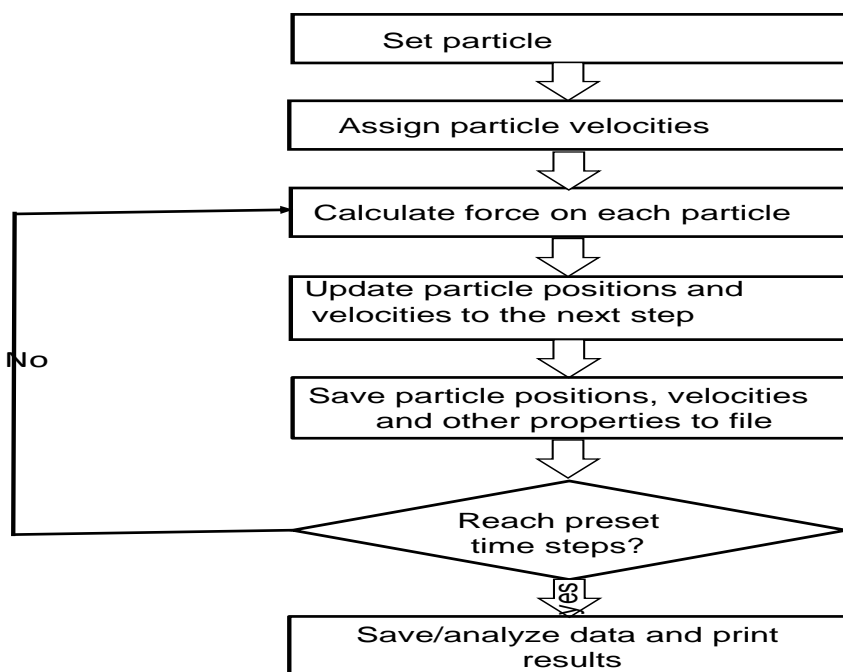


Figure 2.3 schematic representation of various steps involved to calculate the state of atoms in MD simulations

2.5 Molecular Dynamics Ensembles^[31]

The main objective of MD simulation is to replicate a material's structure at atomic scale and predict macroscopic properties without directly depending on experiments. There are different types of ensemble averages used in MD simulation. Among these first three types of ensembles are widely used in MD simulations. Based on different conditions these are:

- Constant energy, constant volume (NVE)
- Constant temperature, constant volume (NVT)
- Constant temperature, constant pressure (NPT)
- Constant temperature, constant stress (NST)
- Constant pressure, constant enthalpy (NPH)

An ensemble is a collection of all the possible states of a real system. The micro canonical statistical ensemble (NVE) describes an isolated system with a given number of particles N , a constant volume V , and a constant energy E . Molecular dynamics simulations naturally fit the NVE ensemble because energy is conserved by Newton's equations of motion.

The canonical statistical ensemble (NVT) describes a system with a given number of particles N , a constant volume V , and a constant temperature T (see fig.2.4). The isothermal-isobaric statistical ensemble describes a system with a given number of particles N , a constant pressure P and a constant temperature T . It is the most common ensemble used in molecular simulations, because it reproduces the behaviour of a material in real conditions of pressure and temperature. The micro canonical or constant N , V , and E (NVE) ensemble, the canonical (NVT) ensemble (see fig.2.4), and the isothermal-isobaric (NPT) ensemble (see fig2.4) are commonly used in MD. The abbreviations N , V , E , T , and P stand for the number of atoms, volume, energy, temperature, and pressure of the system, respectively and these quantities are kept constant during the simulation. As an example, the number of atoms, temperature, and pressure are constant in the NPT ensemble.

The goal of molecular dynamics simulations is to provide information about the physical properties of a macroscopic system. A difficulty to overcome in these calculations is that they are computationally time consuming, limiting in most cases the size of the simulated system to only a few thousands of particles. This number is clearly far from the thermodynamic limit; for such small systems it cannot be safely assumed that the choice of the boundary conditions has a negligible effect on the properties of the system. In order to simulate bulk phases it is essential to choose boundary conditions that mimic practically an infinite sample of the material. This

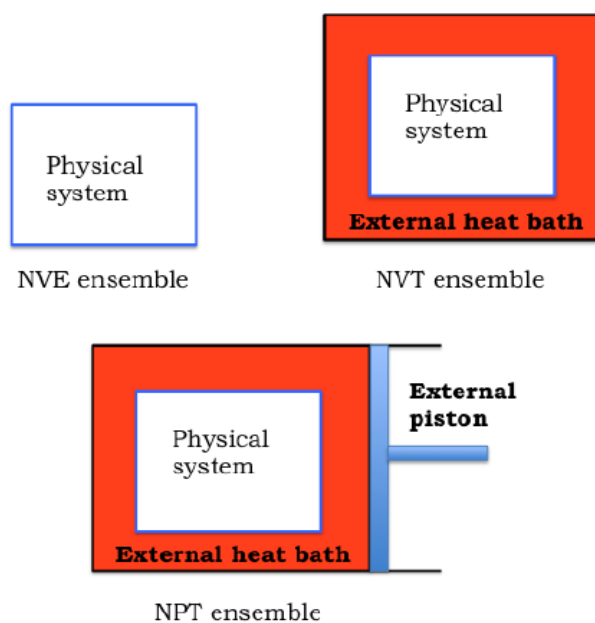


Figure 2.4 Graphical representation of constant NVE, NVT and NPT ensemble [31]

is usually achieved by employing the so called periodic boundary conditions.

2.6 EAM Potential^[32]

The accuracy of any molecular dynamics based simulation ultimately depends on the potential employed to represent atomistic interactions. The force matched embedded atom method (EAM) potential proposed by Fellingner et al. [33] has been employed in this work. The EAM potential has been well-established for use in atomistic simulations of metals and alloys, and a variety of interatomic potentials based on EAM have been devised and validated against either experimental or higher fidelity modelling data. EAM potentials overcome limitations of pairwise interactions of interatomic potentials. Pairwise wise interactions of interatomic potentials yield a number of wrong predictions for transition metals. The EAM potential consists of two terms:

- 1.) A many body term that represents the interaction between the atom and electron cloud of the surrounding atoms
- 2.) A pair wise interaction term that represents the interaction between the atom and its neighbours. Mathematically the EAM potential is given by

$$E = \sum_i F_i(n_i) + \sum_{i<j} \phi_{ij}(r_{ij}) \quad (1)$$

Where;

E = overall potential energy of an atom,

n_i = electron density,

F_i =the embedding energy and

ϕ_{ij} = the component representing the pair wise interaction.

$r_{ij}=|r_i - r_j|$, distance between atoms i and j

In the EAM potential proposed in the paper, the three functional forms (F_i , n_i and ϕ_{ij}) were determined by optimizing parameters to a well converged set of energies, forces and stresses by employing density functional theory (DFT). DFT computational modelling technique used various fields such as in material science to investigate the electronic structure (at the ground state of many body atoms. With this theory the properties of many -electron systems can be calculated.

For the present research application, it is desired that the potential accurately reproduces the elastic constants, cohesive energy, stacking fault energy and point defect migration. To

investigate the effects of radiation on the mechanical and fracture properties of a single crystal of niobium, simulations were initiated by imparting low kinetic energy (≤ 1 keV) values to one of the atoms for generating displacement cascade or point defects. As lower energy PKA (≤ 1 keV) has been used in all the simulations, no modification has been performed in the equation of EAM potential to account for the strong repulsive interaction not represented by EAM that would occur as a result of close approach between atoms. The strong short-range repulsive term is not included with the EAM potential because at low values of PKA energies (≤ 1 keV), the interatomic repulsion due to the embedding term in the EAM is sufficient to shield the nucleuses of two atoms from the short range repulsion experienced by higher energy atoms. Also at such low PKA energies this potential was well tested and validated for estimating the migration of point defects in niobium.

2.7 Validation of EAM Potentials

It is very important to validate the potential in order to understand the results obtained from the various simulations are within the acceptance level or not. For this simulations were performed on LAMMPS (large scale atomic/ molecular massively parallel simulator), dimensions of the simulation box with the periodic boundary conditions in all the three directions were kept fixed at 30Å x30Å x30 Å. Size of the simulation box was kept large enough to avoid any image interactions between the defects generated even with the highest energy PKA ($\approx 1\text{keV}$). A NPT ensemble (constant atoms, pressure and temperature) consisting of 128,000 atoms, 300°K temperature.

2.8 Validation of Young's Modulus with the Help of MD Simulations Using Energy Method

Strain energy between the interacting atoms during the simulations due to EAM potential can represented as the difference between the strain energy at the various time steps (.001 ps) and the initial strain energy due to equilibrium conditions achieved by applying NPT ensemble.

$$U = E - E_o$$

Where;

E= strain energy at various time steps

E_o=strain energy at equilibrium condition.

In the fig.2.6 on the y-axis strain energy has been plotted and on x-axis strain has been plotted. In order to get the most accurate results higher order (order 3) polynomial expression is obtained by curve fitting using various data points produced from the simulation.

$$\text{strain energy} = \frac{1}{2} \text{stress} * \text{strain} * \text{volume}$$

$$u = \frac{1}{2} \sigma * \epsilon * V_o \quad 1$$

$$u = \frac{1}{2} E * \epsilon^2 * V_o \quad 2$$

$$\frac{\partial u}{\partial \epsilon} = E * \epsilon * V_o \quad 3$$

$$E = \frac{\partial^2 u}{\partial \epsilon^2} * \left(\frac{1}{V_0}\right)$$

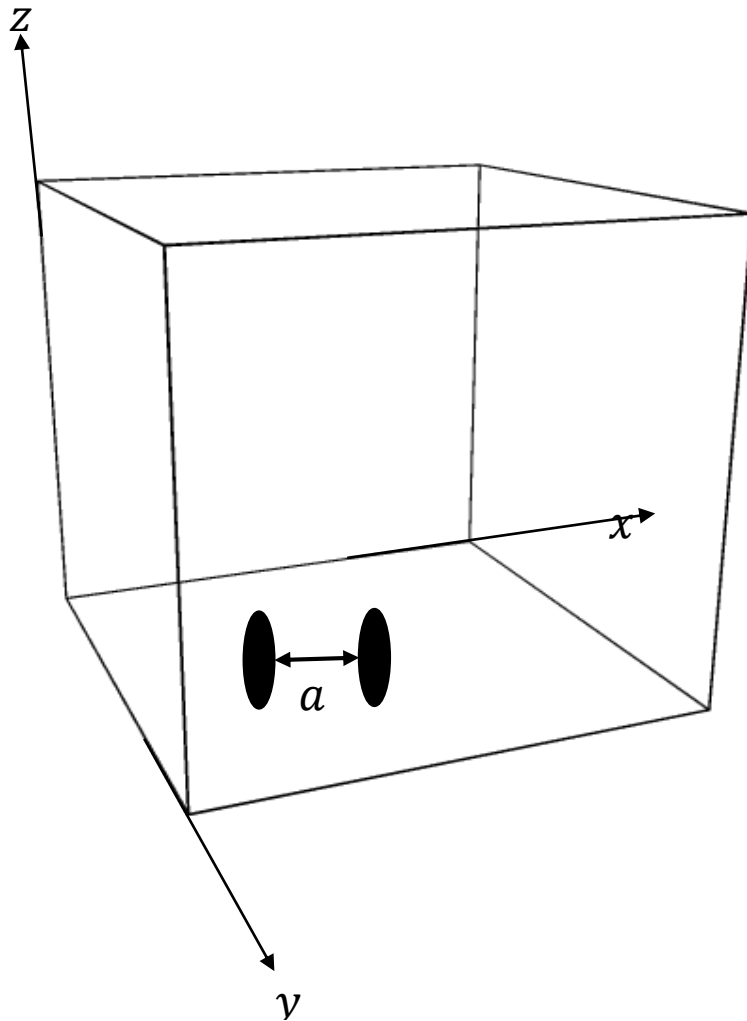


Figure 2.5 simulation box with two atoms (OVITO), total simulation box size is calculated as the distance between the two atoms multiplied by box length in particular direction ('a' is lattice constant for Nb $a=3.308\text{\AA}$).

Where;

σ = stress (GPa)

$\frac{\partial u}{\partial \epsilon}$ =variation of strain energy w.r.t strain and

V_0 = initial volume of the simulation box.

From the fig2.6 the total amount of energy can be expressed as

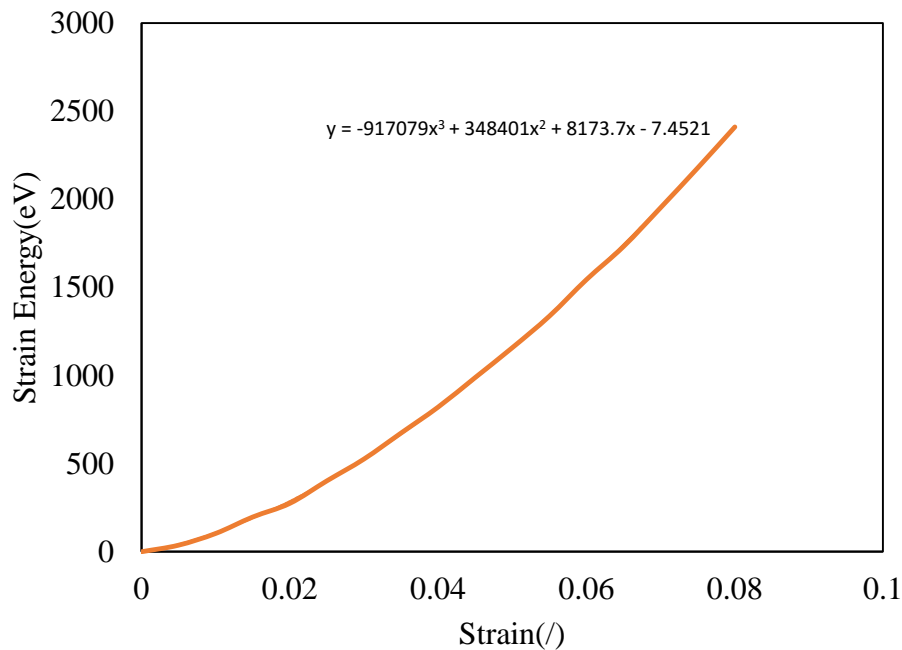


Figure 2.6 strain energy vs strain graph in order to validate EAM potential

$$y = -917079x^3 + 348401x^2 + 8173.7x - 7.4521$$

Using the relations of equations 1&2, differentiating eq (3) once we will have;

$$E = \frac{2 * 348401 * 1.6021 * 10^{(-19)}}{(3.308 * 30 * 10^{-10})^3}$$

The value of Young's Modulus (E) =114.219 GPa

In order to validate the value of young's Modulus simulations were carried at different temperature conditions. The values of strain energy is obtained using equation 1&2. All the simulations were carried at NPT ensemble the box size was kept constant 30Åx30Åx30Å, time step .001 ps and number of atoms 1, 28,000.

Table 2.1 validation of Yong's Modulus by varying simulation temperature.

S.No.	Strain energy equation	Value of young's Modulus(E)
1.) 100 K	$y = -226447x^3 + 51847x^2 + 1314x - 25.743$	115.56 GPa

2.) 200 K	$y = -176858x^3 + 35010x^2 + 2691.2x - 42.827$	117.68 GPa
3.) 450 K	$y = -80946x^3 + 4111.4x^2 + 5072.7x - 70.799$	118.43 GPa
4.) 600 K	$y = -80946x^3 + 4111.4x^2 + 5072.7x - 70.799$	118.43 GPa

The accuracy of the molecular dynamics based simulations depends upon the various parameters-

- 1.) Type of potential used in the simulation
- 2.) Thermostat conditions applied for simulations
- 3.) Barostat conditions applied for the simulations
- 4.) Ensemble.

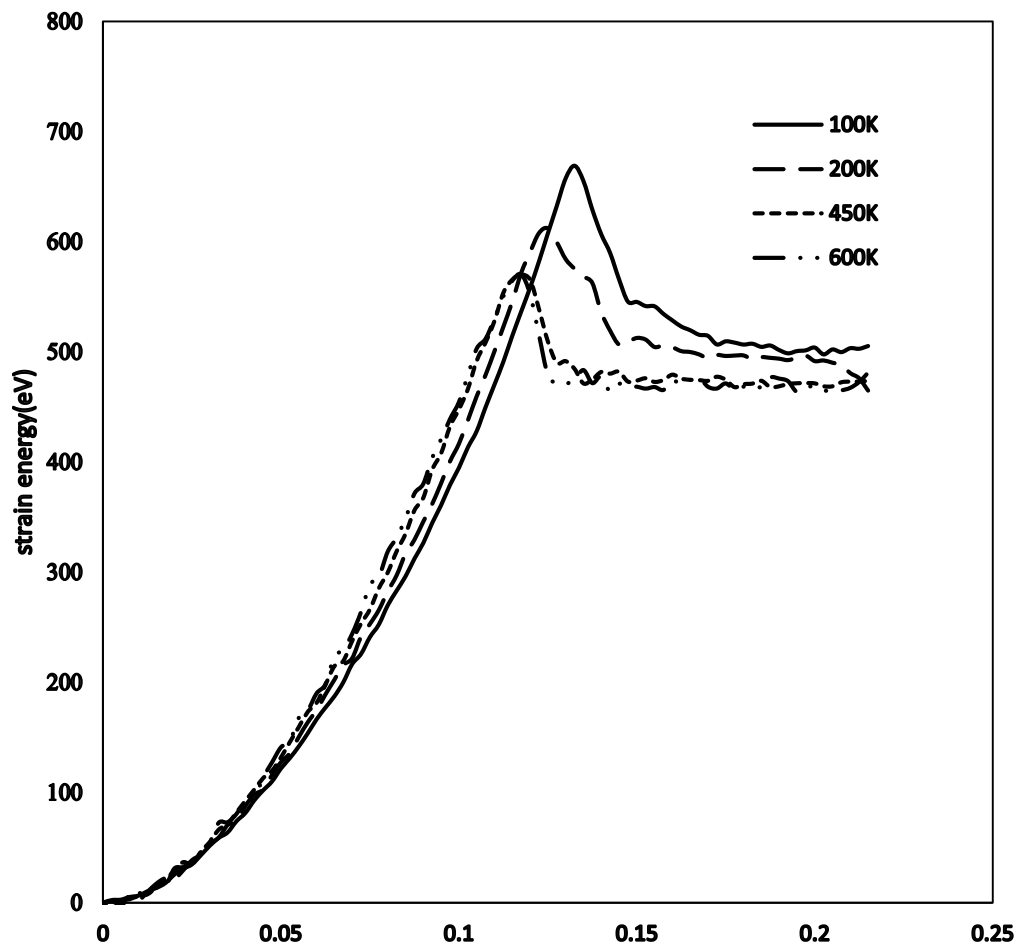


Figure 2.7 strain energy variation w.r.t to simulation box temperature. (Data collection from LAMMPS dump files all simulations were carried out at NPT ensemble).

From the above results it has been observed that the results obtained at NPT ensemble and using NOSE HOOVER thermostat and barostat results obtained are at acceptance level. From the fig.2.7 and table 2.1 it has been observed the value of Young's Modulus and yield point are temperature dependent property. The value of strain energy is maximum at 100 K temperature and is minimum at 600 K.

2.9 Effect of Temperature on Behaviour of Niobium-

In order to investigate the behaviour of the behaviour of Niobium under various temperature conditions simulations were performed at different temperature conditions. NPT ensemble, periodic boundary conditions and size of simulation box was kept constant i.e. $30\text{\AA} \times 30\text{\AA} \times 30\text{\AA}$.

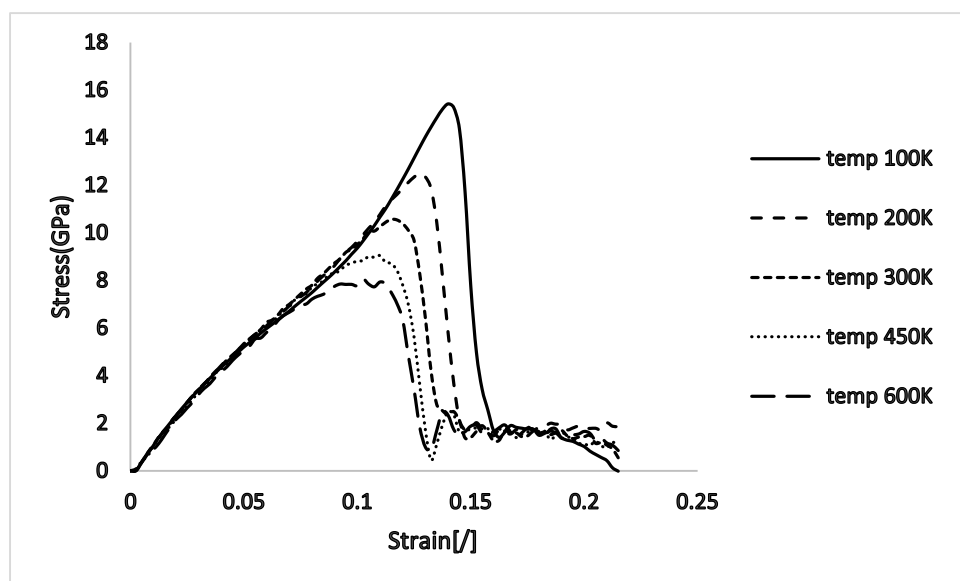


Figure 2.8 stress-strain graph at different temperature conditions

Important results

Temperature variation is having a strong influence on the mechanical behaviour of Niobium. It is clear from fig.2.8, yield point decreases with increase in temperature and vice versa. Up to elastic region material behaviour is less influenced by the temperature but after the elastic region there is drastic change in the behaviour of material. With increase in temperature

slipping of atoms starts because atoms are at higher energy level so the yield point shifted below.

2.10 Effect of Simulation Box on the Mechanical Behaviour of Niobium

In continuation to understand the behaviour of niobium material simulations were performed at various box sizes. The simulation box temperature was kept constant i.e. 300 K and number of atoms in the simulations box was 1, 28,000, NPT ensemble and periodic boundary conditions were applied.

Important result

In the fig.2.9 the stress-strain behaviour by varying simulation box has been shown. With the graph it is clear that there is a negligible influence of box size variation on the stress strain graph. The curve almost resembles from elastic region to yield point. There is a small influence of box size in the breaking point,

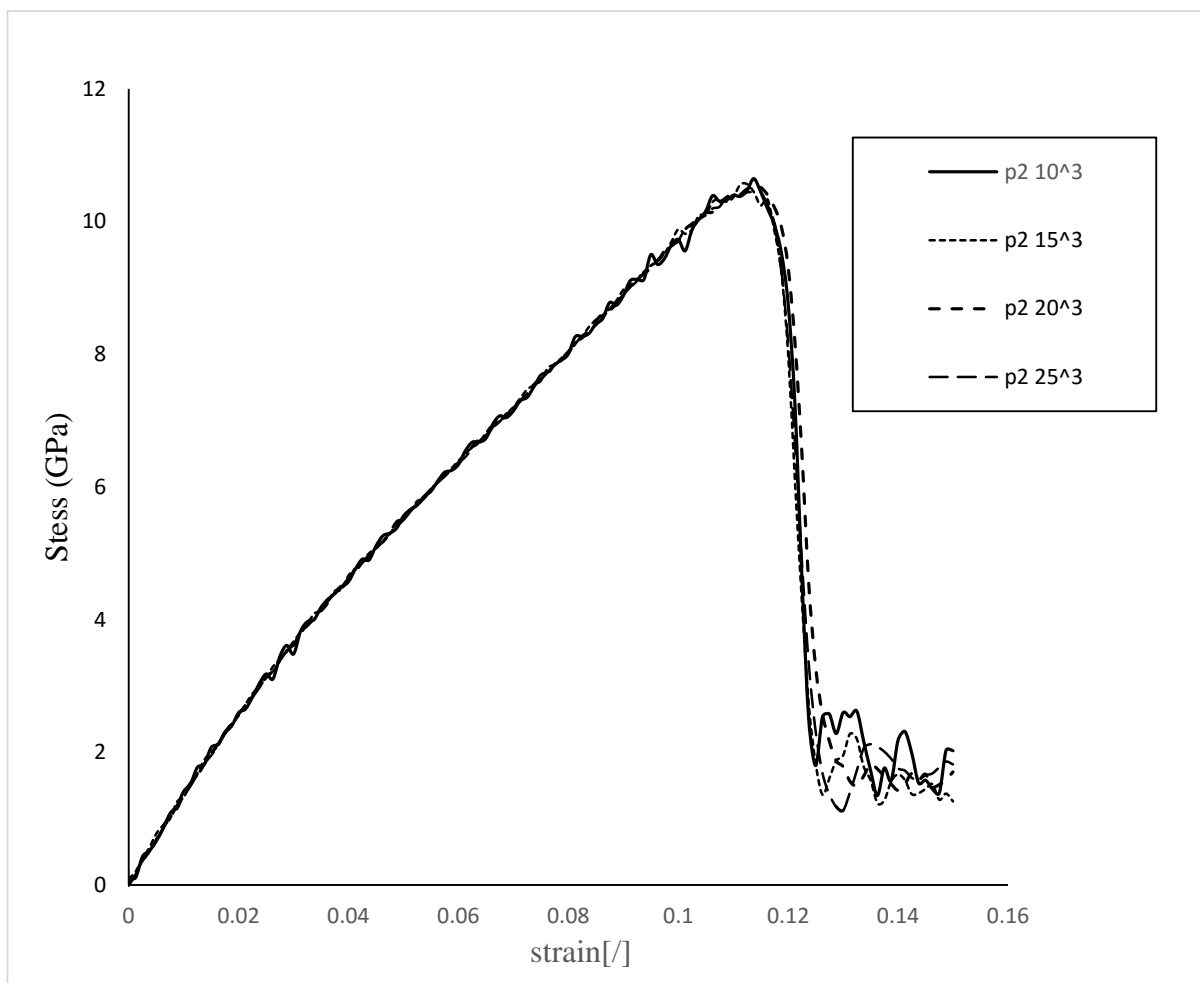


Figure 2.9 stress strain graph by varying simulation box size.(p2 stands for stress in GPa at corresponding simulation box size $10\text{\AA}\times 10\text{\AA}\times 10\text{\AA}=10^3$ and so on.

CHAPTER 3

EFFECT OF DEFECT ON MECHANICAL PROPERTIES OF NIOBIUM

3.0 Introduction

Molecular dynamics (MD) based computer simulation provides a powerful method to study displacement cascades and its impact on material properties. MD examines the classical many body problem for a set of particles interacting through a given interatomic potential. MD has the advantage that the spatial and temporal evolution of the atoms in the simulation box may be followed down to the level where the system has regained thermal equilibrium with its surroundings (≈ 10 ps) and hence can provide insight into important chemical and solid-state-diffusion processes that control the primary state of damage in many irradiated materials.

Molecular dynamics based simulations were performed to understand the behaviour of single crystal Niobium at different conditions (i.e. different PKA direction, different temperature, and different PKA energy). In the fig.3.1 various stages of simulation displacement cascade have been shown, at stage 1 number of atoms have been shown just before the influence of PKA energy all the atoms are at their equilibrium position, at stage 2 due to influence of PKA energy there is a displacement cascade in the simulation box atoms got kinetic energy and they move from their initial position, at stage 3 atoms try to come back to their original position this stage is just after the peak of ballistic phase, at stage 4 some atoms are permanently placed at some position i.e. called self-interstitials and this stage is relaxation stage or phase.

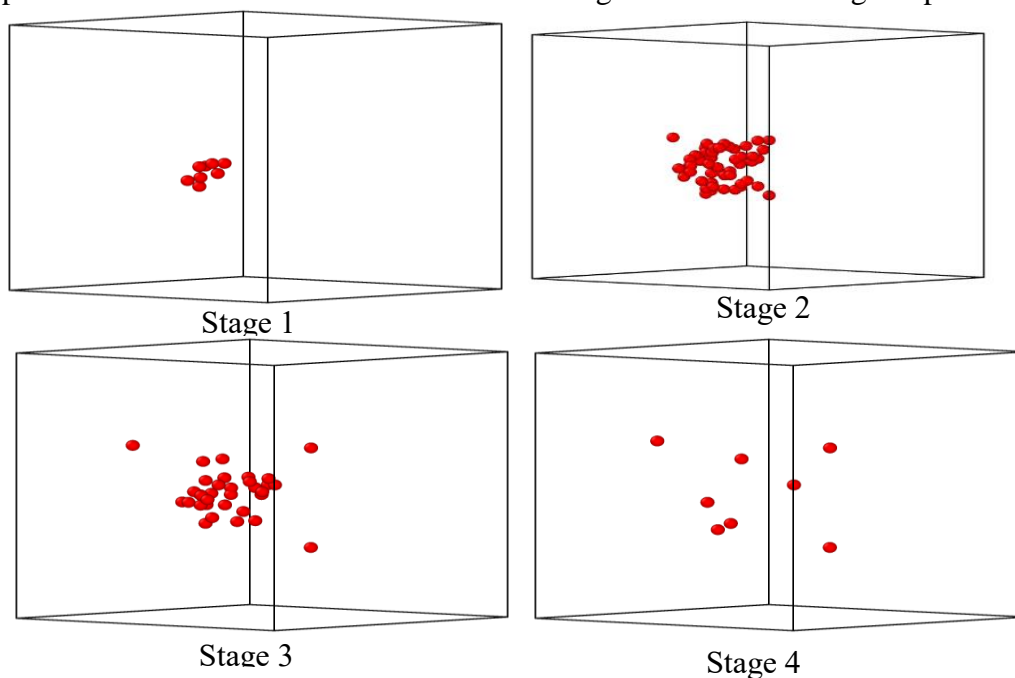


Figure 3.1.1 vacant sites at four stages in the evolution of 1 keV cascade in Niobium at 300 K.

In 3.1.2 number of Frenkel pair's variation w.r.t. to simulation time has been shown. It has

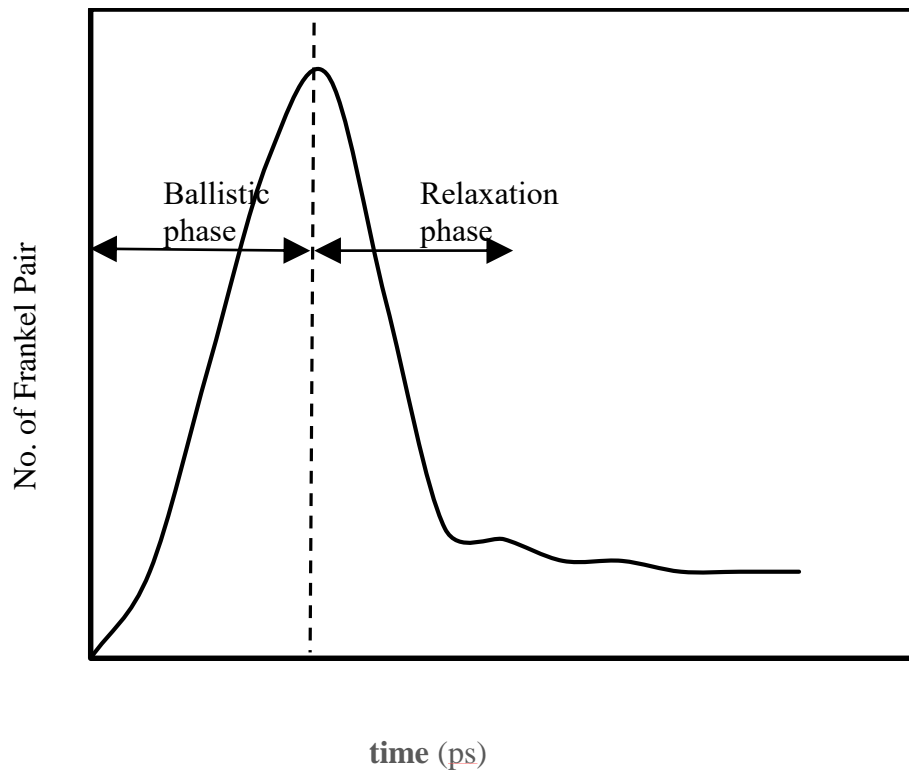


Figure 3.1.2. of Frenkel pairs w.r.t. different time steps

been noticed from various simulations that cascades exhibit two main stages as they evolve with time. The first is a ballistic (or collisional) phase lasting a few tenths of a ps for cascade energies of a few keV, in this duration the PKA energy is distributed among the atoms with the collisions, with the result many atoms leave their lattice sites and another one is relaxation phase some atoms are permanently displaced from their parent sites. These stages are explained below.

3.1 Ballistic Phase

During the ballistic phase of a simulation, the PKA sets up an avalanche of atomic collisions, the total kinetic energy level of the atoms reaches a minimum and the potential energy level a maximum. It is characterised by a rapid increase in the number of atoms displaced from their lattice sites as the shock wave from the 'explosive' cascade core moves outwards [34]. Number of Frenkel pairs is maximum at t_{peak} . Ballistic phase is unstable phase and atoms are at maximum energy level at this stage

3.2 Relaxation Phase

In fig. no 3.1.2 relaxation phase has been shown. In the second phase that lasts several ps, kinetic and potential energy components of crystal energy attain equilibrium with each other. Some atoms leave their parent sites permanently and are responsible for defects in the crystal structure. During relaxation phase majority of the displaced atoms in the outer regions return to their lattice site by thermal relaxation. The atoms not able to regain lattice sites during final stage are responsible for interstitials and vacant sites.

3.3 Effect of Irradiation on Niobium

3.3.1 Effect of Temperature

Simulations to generate displacement cascade has been performed at different set of simulation box temperatures. In order to investigate the impact of temperature on defect generation, a series of simulations were performed with temperatures ranging between 300 K to 600 K. In each simulation, PKA direction and its energy were kept fixed at [135] and 1.0 keV respectively. Average number of defects (vacancy or interstitial) taken from fifteen random simulations are shown in Fig.3.2. The results plotted in Fig.3.2 show that temperature slightly impacts the equilibrium number of defects in a single crystal of niobium. Small increase in number of defects can be observed at a lower temperature of 300°K, but with the increase in

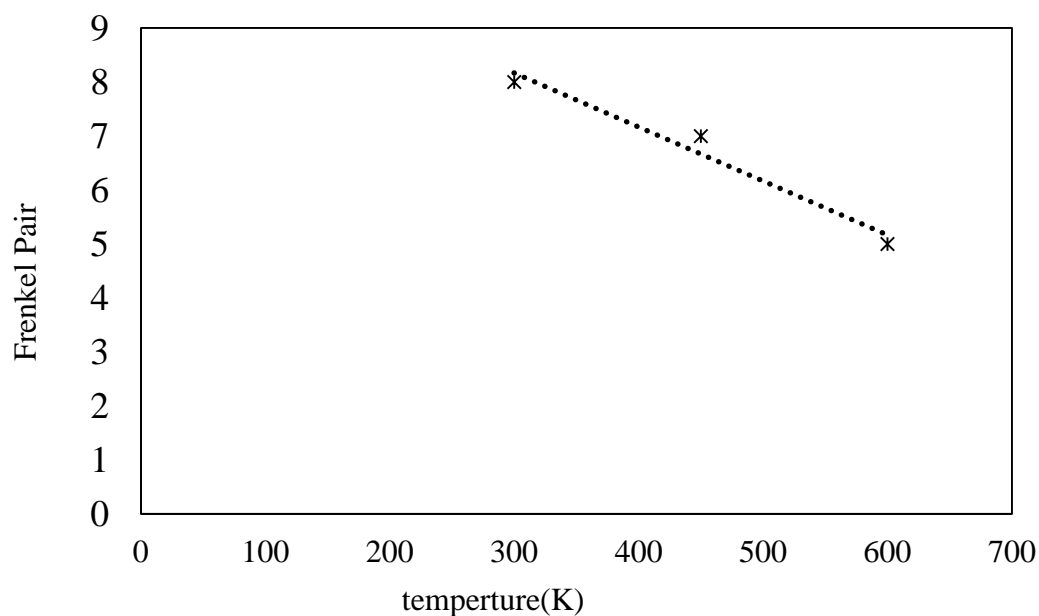
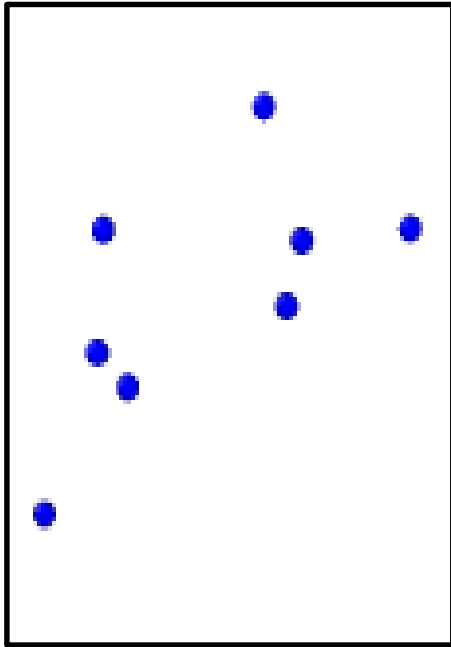
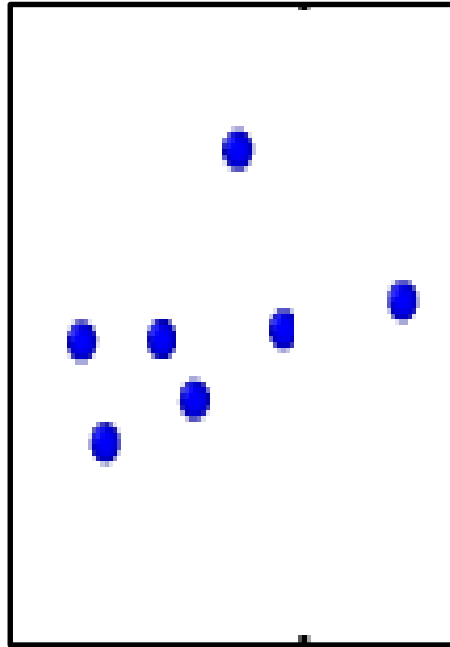


Figure 3.2 Defective atomic sites generated in molecular dynamics based simulation with respect to simulation box temperature

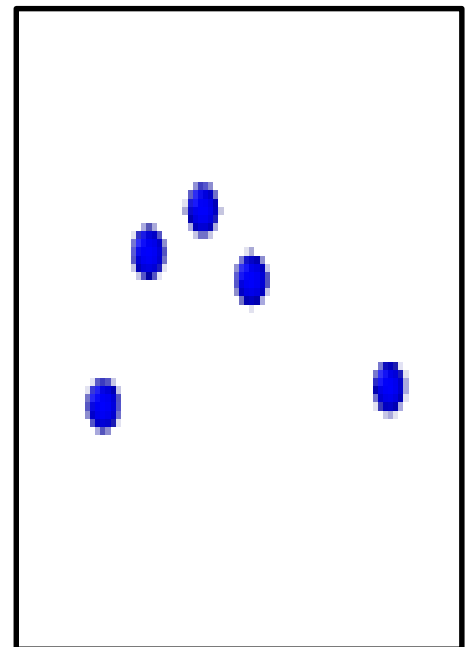
temperature frenkel pair reached a minimum level. On the plotted scale in Fig.3.2 the impact of temperature on defect production can be considered as almost linearly decreasing.



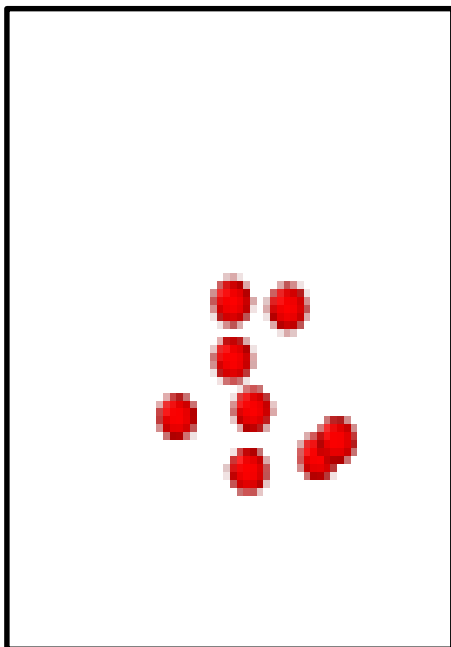
(a) Interstitials 300 K



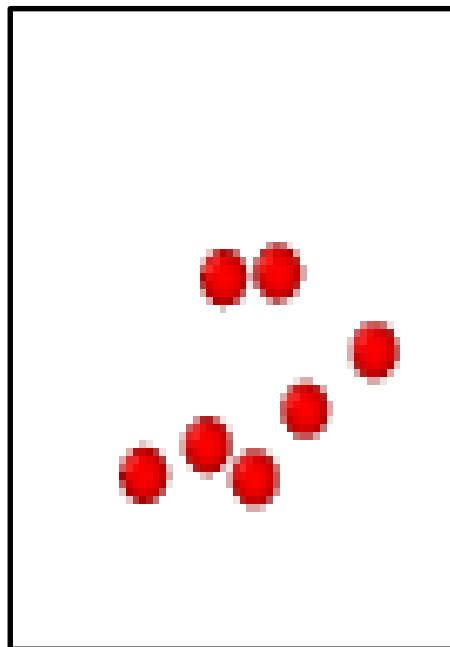
(b) Interstitials 450 K



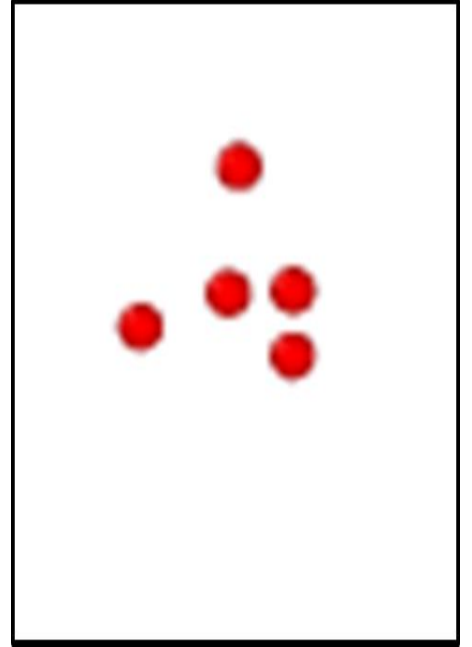
(c) Interstitials 600 K



(d) Vacancy 300 K



(e) Vacancy 450 K



(f) Vacancy 600

Figure 3.3 Distribution of defective atomic sites in the simulation box with respect to a different simulation temperatures of 300°K, 450°K and 600°K.

Important results

- 1) Maximum number of defects has been observed at 300 K temperature.
- 2) At higher temperature number of defects are minimum i.e. at temperature 600 K.
- 3) At lower temperature vacancy are at cluster form and defective atomic sites are close to each other.
- 4) As we increase the temperature of simulation box number of vacancies decreased and distributed in small portion of the crystal structure.
- 5) Atoms at higher temperature are having more chances to get back to their original position and number of defective atomic sites is minimal at higher temperature.

3.3.2 Effect of PKA Direction

Defects generated due to irradiation also depends on the direction of PKA with respect to crystal orientation. Simulations were performed with different PKA directions and number of frenkel pairs along with the distribution of defects has been studied. Simulations were performed with [110], [111], [112] and [100] principle directions and averaged defects from fifteen simulations are displayed in fig.3.4.

It can be inferred from fig.3.4 that maximum defects has been created with PKA direction [112] and [110] which are also the principal directions in bcc crystals. The maximum density of atoms along the principal directions triggered more damage in bcc crystal. Stress strain response has also been captured with each defects single crystal of niobium as shown in fig.3.5. Maximum variation in the response as compared to pristine niobium is shown by [112] and [110].

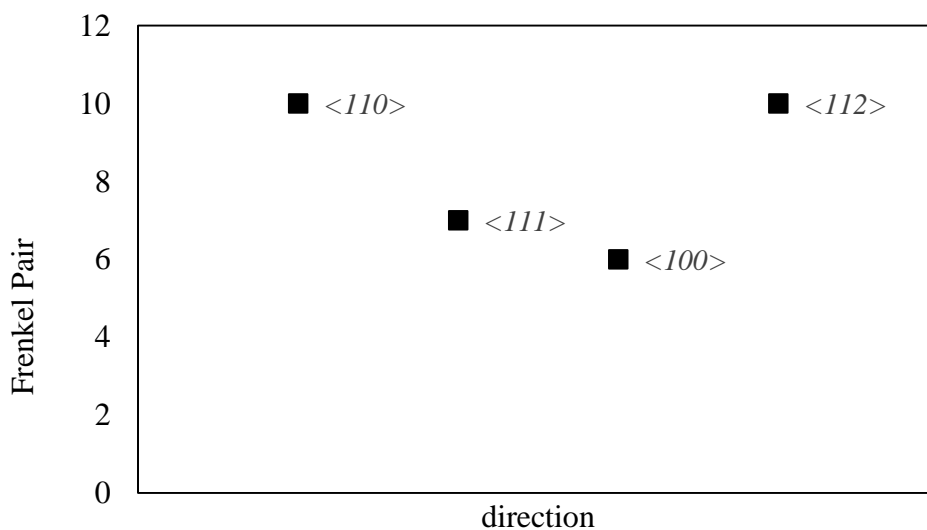


Figure 3.4 distribution of defective atoms at different PKA direction

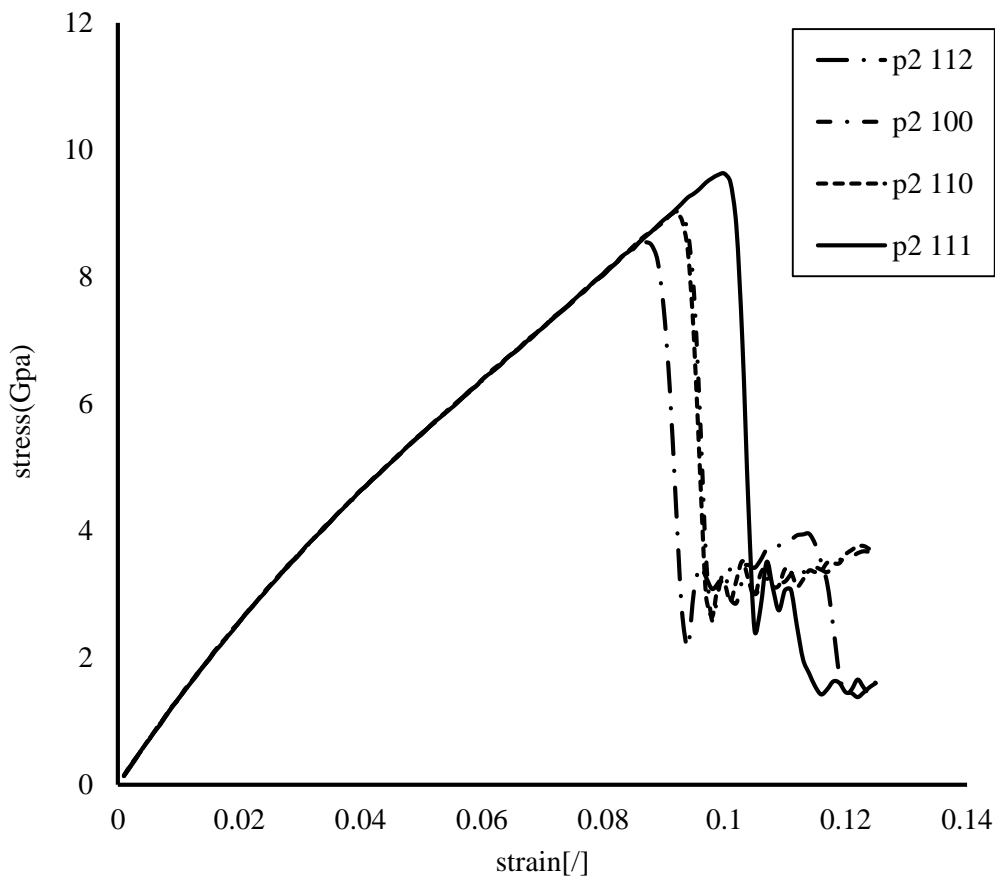


Figure 3.5 stress-strain response at different PKA direction (p2 stands for stress in GPA at corresponding PKA direction)

It can be inferred from the plotted stress strain response in Fig.3.5 that material response to applied load is also affected by the spatial distribution of defects. Triggering of principle slip planes in a single crystal of niobium at the onset of plasticity also depends on the spatial distribution of defects. Effect of spatial distribution of defects on the triggering of slip dislocations is illustrated in Fig.3.6 for the simulations performed with different PKA velocity vectors at a fixed temperature of 300°K. Stress strain response plotted in Fig.3.5 indicated a shift in the onset of plasticity to a lower value of strain with simulations performed with a PKA velocity vector aligned with [112] lattice direction.

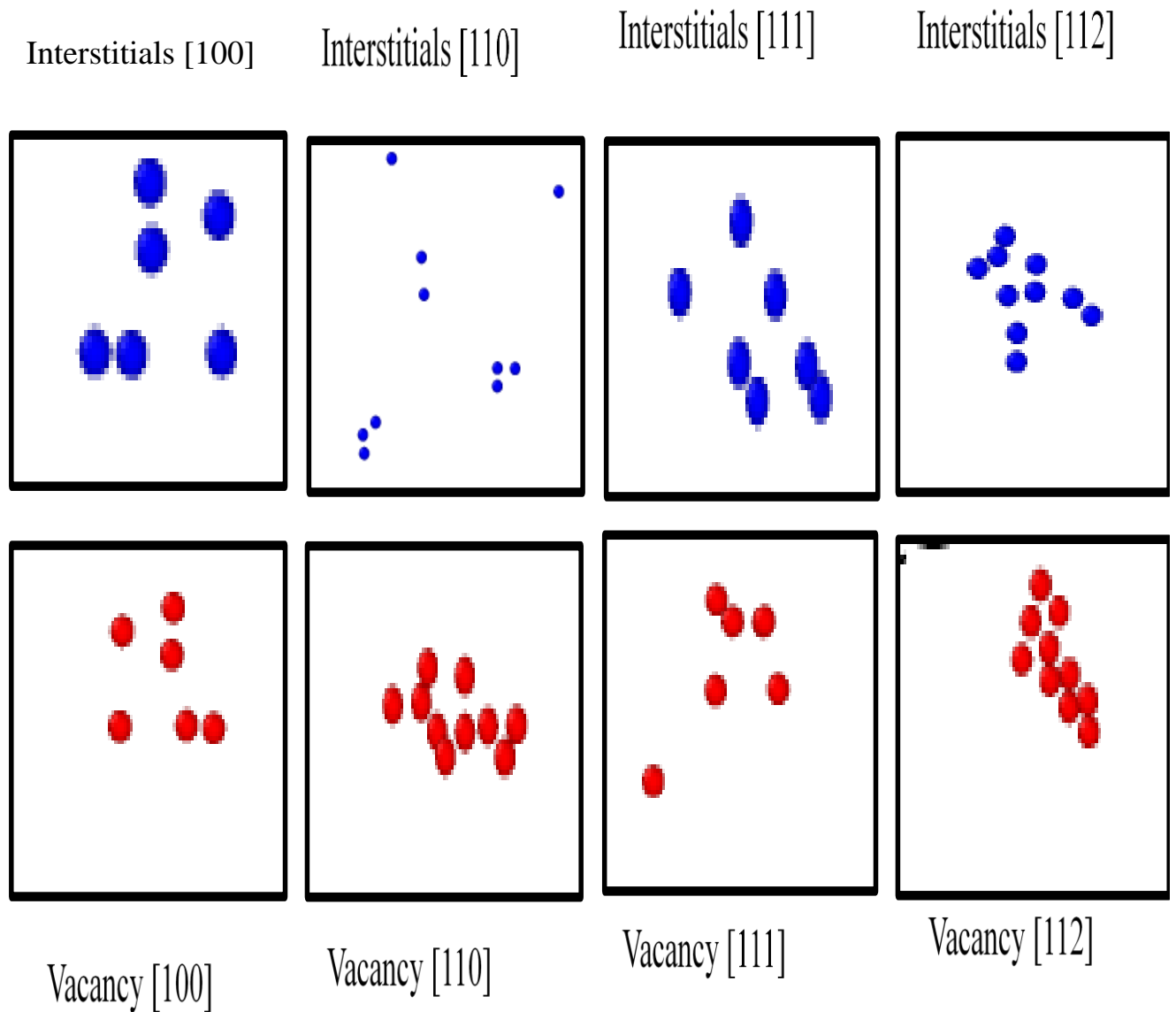


Figure 3. 6 Distribution of defective atomic sites in the simulation box with respect to PKA velocity vector aligned with different crystal orientations at a constant temperature 300 K.

It can also be observed that $\langle 112 \rangle$ and $\langle 110 \rangle$ slip planes acts the principle slip planes in these simulations, which is in accordance with the theory of bcc crystals. These results help in concluding that not only the number of defects and clusters but also their spatial distributions are important for evaluating the change in material properties when subjected to radiation. Spatial distribution of defects is responsible for inducing stress concentration within the single crystal and impacts the overall material response to the applied load.

Important Results-

- 1.) From the fig.3.4 maximum no of defective atomic sites have been seen in $\langle 112 \rangle$ and $\langle 110 \rangle$ direction.
- 2.) Niobium material is of bcc crystal structure, atom density is maximum in principle direction (i.e. $\langle 112 \rangle$ and $\langle 110 \rangle$) so the chances of creating defective atomic sites by PKA velocity vector is higher in these directions.
- 3.) In the above fig.3.6 top four boxes are showing number. of interstitials and bottom four boxes are showing number. of vacancies.

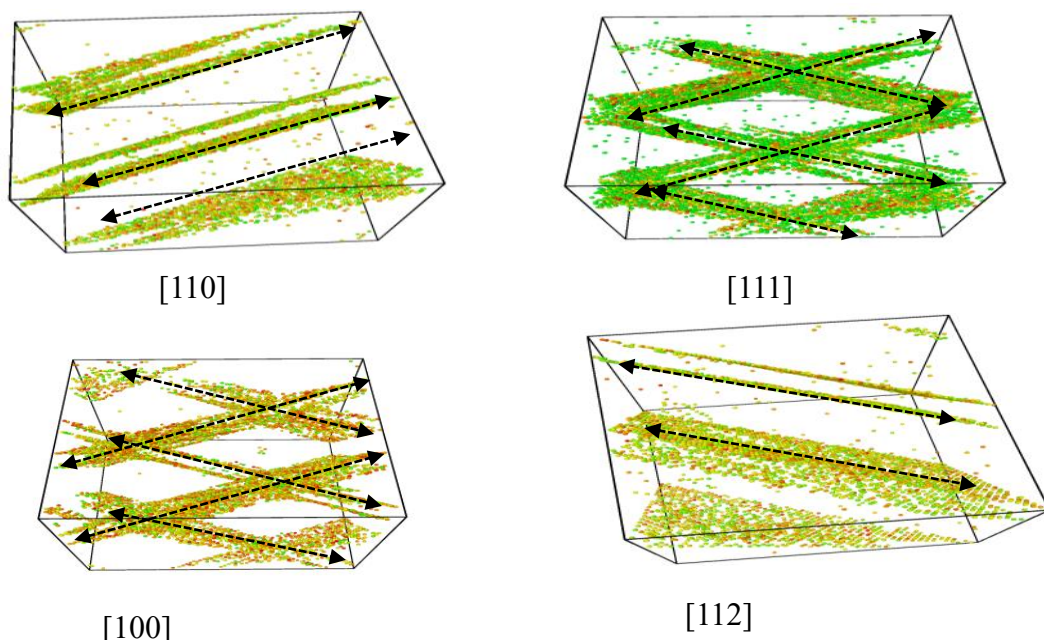


Figure 3.7 Defect distribution and activated slip planes at the onset of plasticity in simulations performed with different PKA directions

In fig.3.6 distribution of defects have been shown with respect to different PKA velocity vectors. In fig.3.7 images corresponds to the initial phase of activated slip planes, and arrows indicating the direction of alignment of principal slip planes. It is shown in Fig.3.7 that spatial distribution of defects obtained from the velocity vectors aligned with lattice direction [100] and [111] triggers cross channelling of slip dislocations, whereas alignment of defects in principal plane $\langle 112 \rangle$ as the case with velocity vector [112], restricts the cross channelling and initiates the early onset of plasticity as indicted in the stress strain response in fig3.14. This

section of simulations helps in concluding that not only the number of defects but also the distribution of these defects in single crystal of niobium is significant to evaluate its materials response to different loading scenarios.

3.3.3 Effect of Energy

MD simulations are used to investigate defect production and direct information on the final number of defective atomic sites and their distribution at various PKA energy. All the simulations were performed at 300K temperature and results have been plotted below. Each energy level simulations were performed for fifteen number of times and average number of defects have been calculated. In fig.3.8 top four boxes are showing number of vacant sites at different PKA energy level and bottom boxes are showing number of interstitials at different PKA energy level.

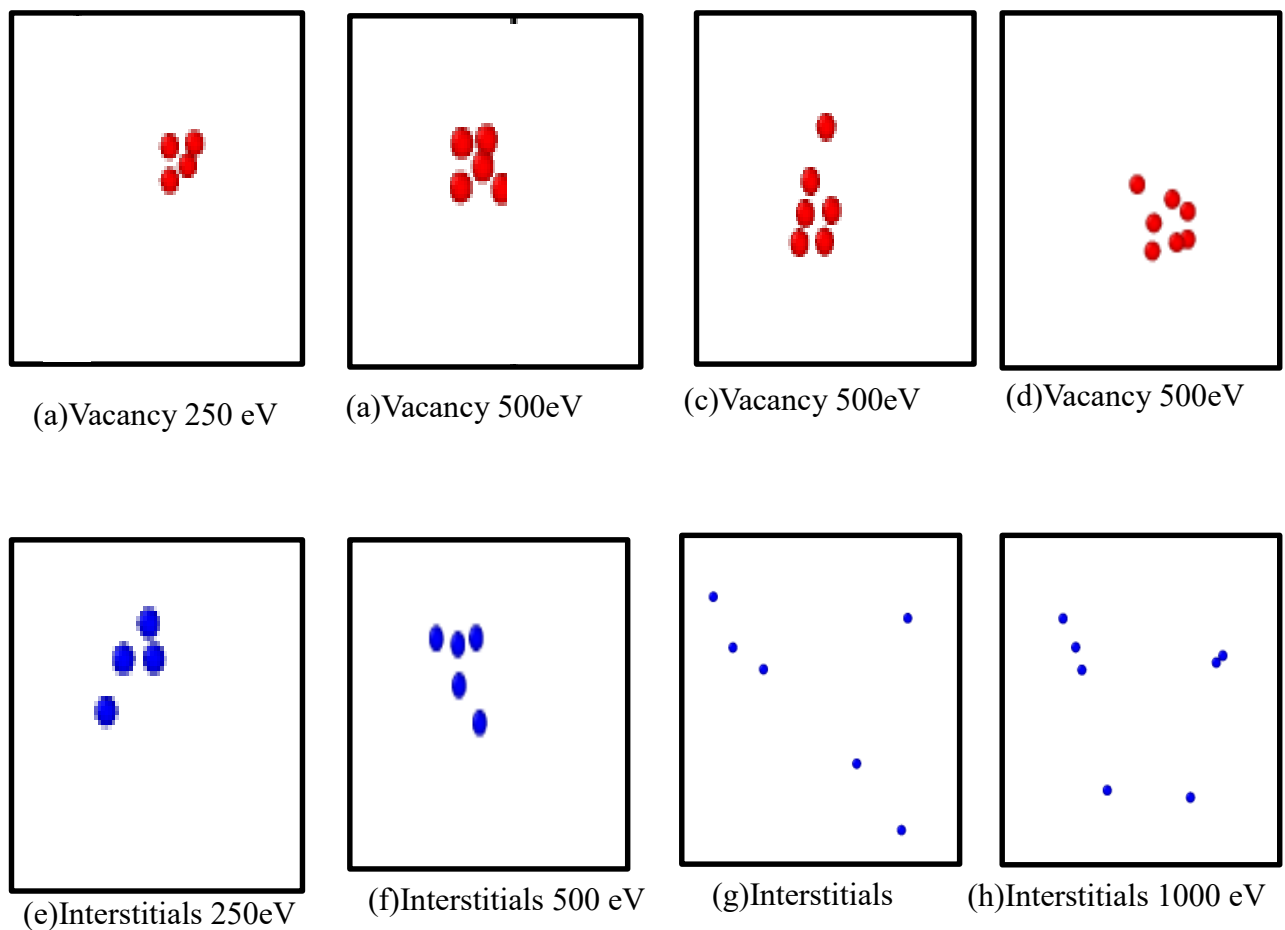


Figure 3.8 Distribution of defective atomic sites in the simulation box with respect to PKA energy.

It can be inferred from fig.3.8 that with the increase in pka energy, defects distribution is also effected. Interstitials are more scatted in simulations performed with higher energy pka, whereas vacancy defects are more crowded and has shown minimum impact of pka energy. Frenkel pairs with respect to pka energy are shown in fig.3.18. The high kinetic energy is generated from the core during the thermal spike and is responsible for creating self-interstitials and vacancies.

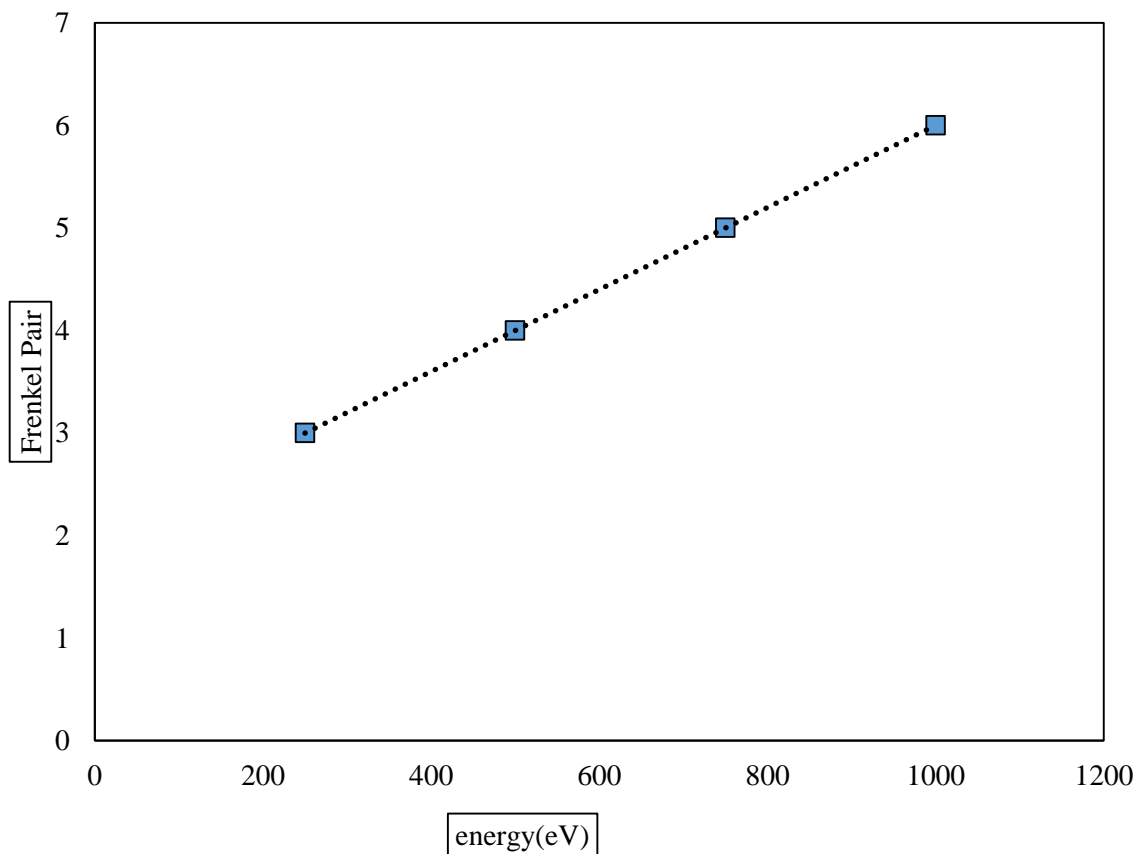


Figure3.9 distribution of defective atoms at different PKA energy.

Important Results and Discussion -

It has been observed that the number of frenkel pairs vary linearly with increase in PKA energy. The geometry of activated slip planes shown in Fig.3.10, Clear channels of slip planes/dislocations without any cross linkage were reported in simulations performed with the

PKA energy of 500 keV and 250 keV at 300°K. Higher density of slip planes with certain amount of cross linkage was reported in .75 keV and 1 keV simulations. In general, cross linkages in slip planes act as a barrier to slip and produce hardening effects in metals. The onset of plasticity at the minimum value of strain in simulations with the PKA energy of .25 keV (refer to Fig.3.10) and PKA energy 0.5 keV was attributed to the absence of cross linkages of slip planes (Fig. 3.10), hence no hardening effect and minimum yield strength as compared to all other cases. It can also be observed that $\langle 112 \rangle$ and $\langle 110 \rangle$ slip planes acts the principle slip planes in these simulations, which is in accordance with the theory of bcc crystals. These results help in concluding that not only the number of defects and clusters but also their spatial distributions are important for evaluating the change in material properties.

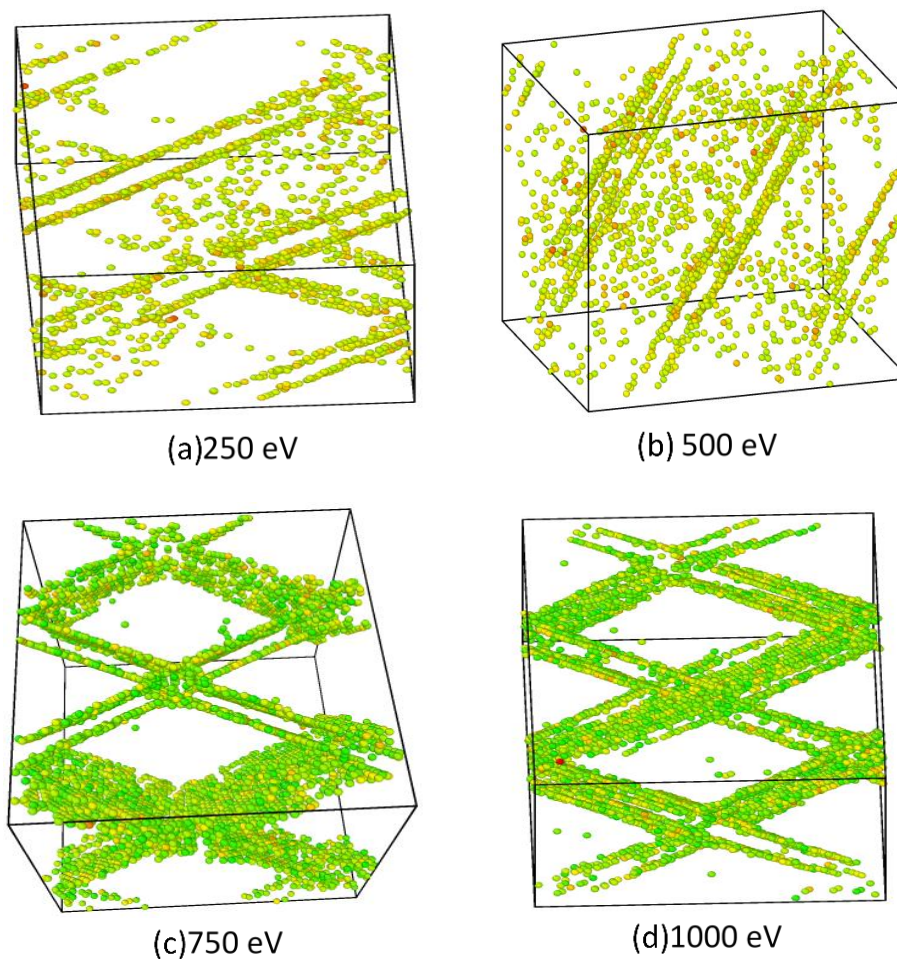


Figure 3.10. Activated slip planes at the onset of plasticity in simulations performed with different PKA energy level at a constant temperature 300K.

Distribution of defects in the crystal structure due to various PKA energy is and their orientations (in fig.3.8), cross channelling of slip planes has been recorded in fig.3.10 (c) and

(d) at higher PKA energy level cross channelling of slip planes is formed. Clear channelling of slip planes/dislocations without any cross linkage were examined in simulations performed with the PKA energy 0.25 keV and 0.50 keV at 300 K. Higher density of slip planes plays an important role to produce hardening effects in metals. These higher density slip planes are barriers to slip planes. These results help in conducting that the defects and their clusters are also affected by different PKA energy. The energy generated from the core due to irradiation is of various keV order, it strikes on the crystal structure and lost in picoseconds causing defects in the crystal structure. These thermal spikes are responsible for hardening effect in the material.

3.4 Combined Radiation and Loading

It is important to understand behaviour of nuclear shielding material under different loading conditions. As per the concern simulations were performed at uniaxial tensile loading condition and the response of material has been recorded. All the simulations were performed at PKA energy 1.0 keV after equilibrium condition and simulations of irradiation damage was run in conjunction with uniaxial tensile loading. The simulated atom distributions with equilibrium defect distributions were used as input for uniaxial tensile loading simulations (as illustrated graphically in Fig.3.11). This type of simulation is associated high strain rates, causing small time steps in the range of at least pico-seconds. The high values for yield strength reported in this work are only due to high values of strain rate in the range of 10^9 /second. The NPT ensemble was again employed with periodic boundary conditions and, for these studies, the total number of atoms used in the simulation was kept constant at 1, 28,000.

These vacancies and interstitials have been shown in fig.3.11 and activated slip planes geometry due to applied load has been shown in fig.3.12. in Figure 3.11 Distribution of defective atomic sites in the simulation box fig.3.11 (a) distribution of interstitials when uniaxial tensile load is applied and vacancies in fig.3.11(b) distribution of interstitials fig.3.11(c) and vacancies fig.3.11(d) in case only of no external loading. It has been observed that material is having direct impact of loading on material response. Higher density of slip planes with certain amount of cross linkage (see fig.3.12b) was reported in when material is

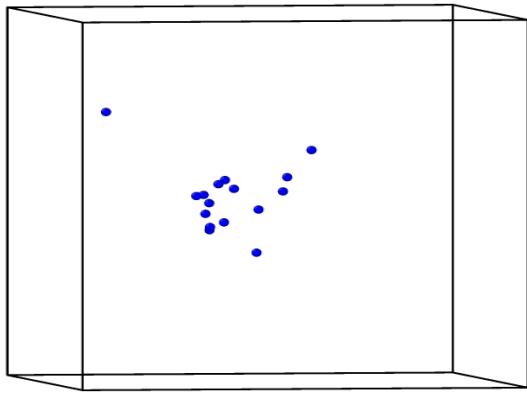


Figure 3.11a

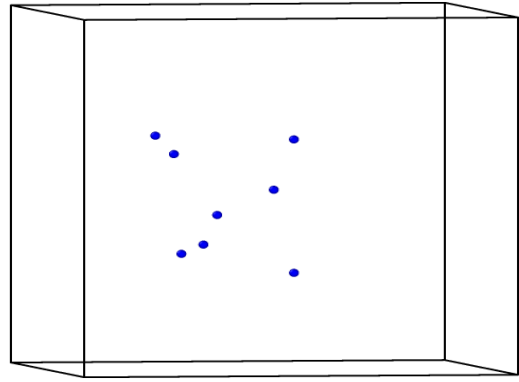


Figure 3.11b

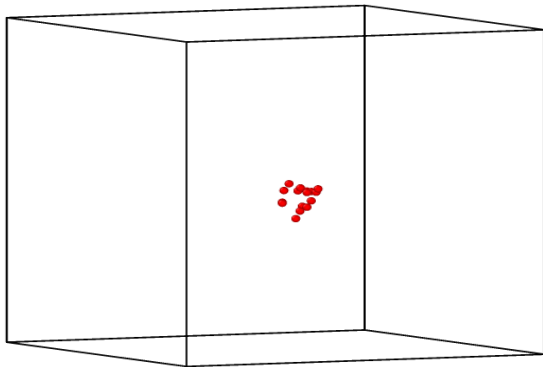


Figure 3.11c

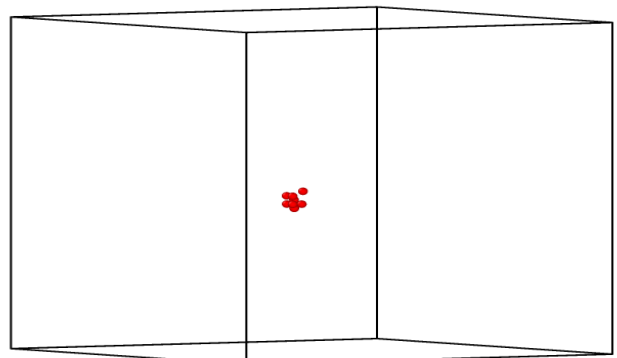


Figure 3.11d

Figure 3.11 Distribution of defective atomic sites in the simulation box (a) distribution of interstitials when uniaxial tensile load is applied and vacancies in (b) distribution of interstitials (c) and vacancies(d) in case only of no external loading

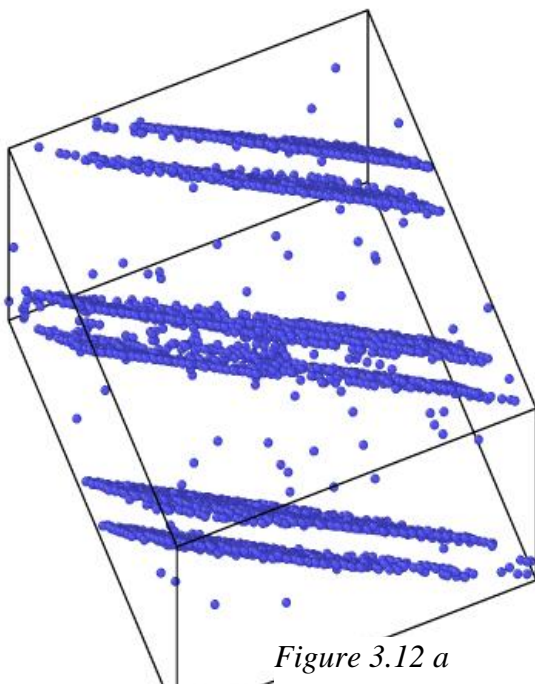


Figure 3.12 a

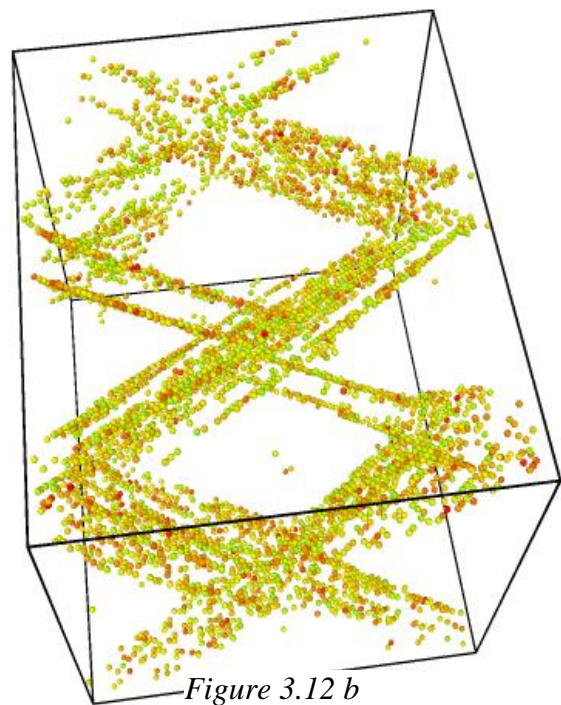


Figure 3.12 b

Figure 3.12 dislocation channelling and activated slip planes at the onset of plasticity in simulations performed with (b) loading and without loading (a).

of plasticity at the minimum value of strain in simulations with the PKA energy of 1.0 keV (refer to Fig.3.12a) was attributed to the absence of cross linkages of slip planes, hence no hardening effect and minimum yield strength as compared to former case.

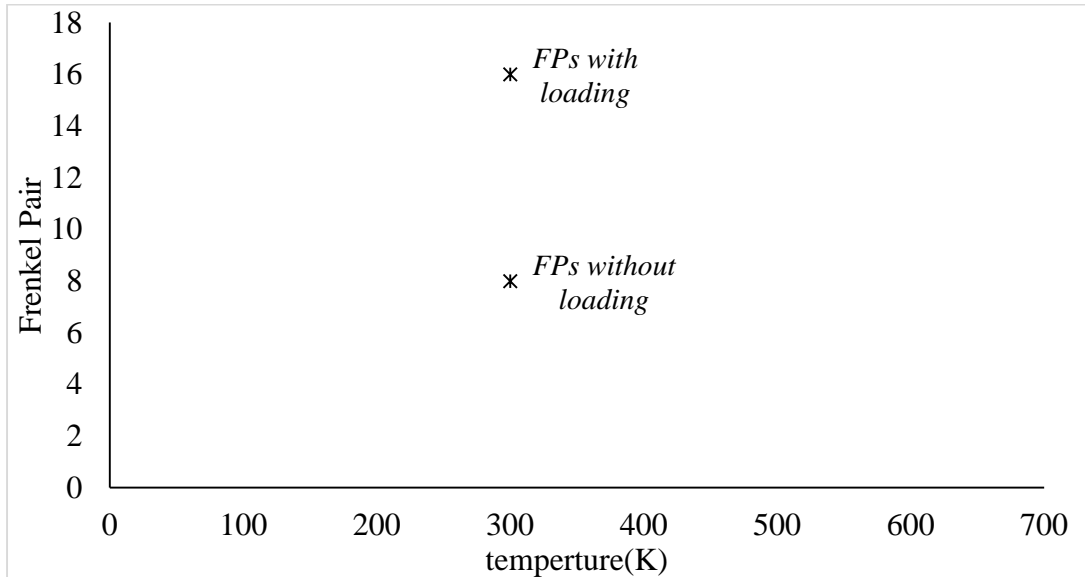


Figure 3.13 number of Frenkel pairs when Niobium single crystal is subjected to uniaxial tensile loading at PKA energy 1 keV and at 300 K temperature.

In fig.3.13 number of Frenkel pairs compared in two cases i.e. when the material under direct impact of incident radiation and in another situation, in addition of radiation induced damage, uniaxial tensile load applied. To compare both case the simulations temperature was kept same i.e. 300 K, box size

Important Results and Discussion –

- Number of defective atomic sites depends upon applied load on the material.
- Number of vacancies and interstitials are increased due to applied loading (see fig 3.22 number of Frenkel pairs become twice).
- Activated slip planes in (fig.3.21a) are formed due to incident PKA energy, cross channelling of slip planes (fig3.21b) formed due to combined loading effects.

Conclusion

Molecular dynamics based simulations helped to validate the different properties of Nb by using molecular mechanics (MM)EAM potential field, cohesive energy, Young's modulus, lattice constant with the help of LAMMPS.

Maximum number of defects has been observed at 300 K temperature at higher temperature number of defects are minimum i.e. at temperature 600 K t lower temperature vacancy are at cluster form and defective atomic sites are close to each other. As we increase the temperature of simulation box number of vacancies decreased and distributed in small portion of the crystal structure.

Niobium is having bcc crystal structure and atom density is maximum in principle direction so maximum number of defective atomic sites were observed in principle direction of bcc crystal.

Number of frenkel pairs vary linearly with increase in PKA energy. The geometry of activated slip planes forming clear channels without any cross linkage. Higher density of slip planes with certain amount of cross linkage was reported in .75 keV and 1 keV simulations.

REFERENCES

1. Wooding, S.J., Howe, L.M., Gao, F., Calder, A.F., Bacon, D.J., 1998, "A molecular dynamics study of high energy displacement cascades in α -zirconium" *Journal of Nuclear Material*, pp. 254, 191-204, 2001.
2. Wooding, S.J., Bacon, D.J., 1997, "A molecular dynamics study of displacement cascades in α -zirconium" vol. 76 page 1033-1051, 11 March 1997.
3. Garry S. Was, "Fundamentals of radiation material science- metals and alloy" Springer –Verlag Berlin Heidelberg 2007. Butler D, "Nuclear power's Dawn" *nature* 429:238-240, 2004.
4. Stoller R.E, Odette, G.R., Wirth, B.D, "Primary damage formation in bcc iron" *Journal of Nuclear Material* 251, 49-60, 1997.
5. Victoria, M., Baluc, N., Bailat, C., Dai, R., Singh, B.N., "The microstructural and associated tensile properties of irradiated fcc and bcc metals" *Journal of Nuclear Material* 276, 114-122, 2000.
6. Fikar J., Schaublin, R., Molecular dynamics simulation of radiation damage in bcc tungsten. *Journal of Nuclear Material* 386-388, 97-101, 2009.
7. Eagleson, M, "Concise encyclopaedia chemistry". Berlin: pp 1199, 1994.
8. Tucker, R.P., Wechsler, M.S., Ohr, S.M., Dislocation channelling in neutron irradiated niobium" *Journal of applied physics*. 40, 400-408, 1969.
9. Williams, B.W., Lawrence, S. St., Leitch, B., "Comparison of the measured and predicted crack propagation behaviour of Zr-2.5Nb pressure tube material" *Engineering Fracture Mechanics*. 78, 3135-3152, 2011.
10. Abraham, F., Brodeck, D., Rudge, W.E., Xu, X., "A molecular dynamics investigation of rapid fracture mechanics." *J. Mech. Phys. Solids* 45, 1595-1649, 1997.
11. Guo. , Y.F., Wang, C.Y., Zhao, D.L., "Atomistic simulation of crack cleavage and blunting in bcc-Fe" *Mater. Sci. Eng., A*. A349, 29-35, 2003.
12. Karimi, M., Roarty, T., Kaplan, T., "Molecular dynamics simulations of crack propagation in Ni with defects" *Modelling Simul. Mater. Sci. Eng.* 14, 1409-1420, 2009
13. Tabar, H.R., Shodja, H.M., Darabi, M., Dahi, A., "Molecular dynamics simulation of crack propagation in fcc materials containing clusters of impurities". *Mech. Mater.* 38, 243-252, 2006.
14. <https://en.wikipedia.org/wiki/Columbite>, Nov. 2015.

15. Ju-Young Kim, Dongchan Jang, Julia R. Greer, “Tensile and compressive behaviour of tungsten, molybdenum, tantalum and niobium at the nanoscale” *Acta Materialia* 58 2355–2363, (2010).
16. Seeger, A. “Proceedings of the second United Nations international conference on the peaceful uses of atomic energy”. Vol.6, 250, 1958
17. Stukowski A., Albe K., “Dislocation detection algorithm for atomistic simulations. Modelling Simulations” *Mater. Sci. Eng.*18, 025016, 2010.
18. S.J. Wooding, L.M. Howe, F. Gao, A.F. Calder and D.J. Bacon, “A molecular dynamics based study of high energy displacement cascades in alpha zirconium” *Journal of nuclear Materials*, vol. 254, issues 2-3, pages 191-204, April 1998.
19. F. Gao, D.J. Bacon, L.M. Howe and C.B. So, “Temperature Dependence of Defect Creation and Clustering by Displacement Cascades in α -Zirconium” *Journal of nuclear Materials*, vol. 294, issue 3, pages 288-298, April 2001.
20. Rajesh Kumar, G Rajshekharan and Avinash Parashar, “Molecular dynamics based study on boron nitrides nanotubes (BNNS) to see the behaviour of material at tensile loading at atomistic level” IOP publishing, nanotechnology 27 085706 (11pp), January 2016.
21. G. Rajshekharan, Avinash Parashar, “Molecular Dynamics Study on Mechanical Response and Failure Behaviour of Graphene: Performance Enhancement via 5-7-7-5 Defects”. *RSC Advances*,6,26361-26361(2016)
22. Butcher et al, Cindy L. Routree and Priya Vashistha, “Atomistic plasticity: description and analysis of a one billion atom simulation of ductile materials failure”, *Computational Methods Appl. Mech. Engg.* 193 (2004) 5257–5282, 2002.
23. S. Namilae, N. Chandra, T.G. Nieh, “Atomistic simulation of grain boundary sliding in pure and magnesium doped aluminium bi-crystals” *Scripta Materialia* 46 (2002) 49–54.
24. C. Zheng and Y. W. Zhang, “Atomistic simulations of mechanical deformation of high-angle and low-angle nanocrystal line copper at room temperature” *Materials Science and Engineering A* 423 (2006) 97–101.
25. D. Furkay, H. Van Swygenhoven, and P. M. Derlet, “Intergranular fracture in nanocrystal line metals” *Physical Review B* 66 (2002) 060101R.
26. H.C. Anderson, “molecular dynamics simulations at constant pressure and temperature” *the journal of chemical physics*, vol. 72, no. 4, pp. 2384-2393, 1980.

27. H. J. C. Berendsen, J. P. M. Postma, W. F. van Gunsteren, A. DiNola, and J. R. Haak, "Molecular dynamics with coupling to an external bath," *The Journal of Chemical Physics*, vol. 81, no. 8, pp. 3684-3690, 1984.
28. P. H. Hnenberger, "Thermostat algorithms for molecular dynamics simulations," *Advanced Computer Simulation*, vol. 173, no. 173, pp. 105149, 2005.
29. D. J. Evans and B. L. Holian, "The nose-hoover thermostat," *The Journal of Chemical Physics*, vol. 83, no. 8, pp. 4069-4074, 1985.
30. G. J. Martyna, D. J. Tobias, and M. L. Klein, "Constant pressure molecular dynamics algorithms" *The Journal of Chemical Physics*, vol. 101, no. 5, pp. 4177-4189, 1994.
31. Nuwan Dewapriya, Mallika Arachige, "molecular dynamics based study of effects of geometric defects on the mechanical properties of graphene" B.Sc. University of Moratuwa, Sri Lanka, 2008.
32. Michael R. Fellingner Hyoungki Park and John W. Wilkins, "Force-matched embedded-atom method potential for niobium" Department of physics, The Ohio State University, Columbus, Ohio 43210, USA, April 2010.
33. H.R. Fellingner, H.Park, J.W. Wilkins, Force matched embedded atom method potential for niobium, *Phys. Rev B: Condens. Matter* 81 (2010) 144119.
34. Dr. Christopher Race, "The Modelling of Radiation Damage in Metals Using Ehrenfest Dynamics" Doctoral Thesis accepted by Imperial College, London, UK, Springer-Verlag Berlin Heidelberg 2010.